BRAIN
ORIGINAL ARTICLE

Activation of the basal ganglia and indirect pathway neurons during frontal lobe seizures

Anastasia Brodovskaya,[1] Shinnosuke Shiono[2] and Jaideep Kapur[2,3]

There are no detailed descriptions of neuronal circuit active during frontal lobe motor seizures. Using activity reporter mice, local field potential recordings, tissue clearing, viral tracing, and super-resolution microscopy, we found neuronal activation after focal motor to bilateral tonic-clonic seizures in the striatum, globus pallidus externus, subthalamic nucleus, substantia nigra pars reticulata and neurons of the indirect pathway.
Seizures preferentially activated dopamine D2 receptor-expressing neurons over D1 in the striatum, which have different projections. Furthermore, the D2 receptor agonist infused into the striatum exerted an anticonvulsant effect. Seizures activate structures via short and long latency loops, and anatomical connections of the seizure focus determine the seizure circuit.
These studies, for the first time, show activation of neurons in the striatum, globus pallidus, subthalamic nucleus, and substantia nigra during frontal lobe motor seizures on the cellular level, revealing a complex neuronal activation circuit subject to modulation by the basal ganglia.

1 Neuroscience Graduate Program, University of Virginia, Charlottesville, VA 22908, USA
2 Department of Neurology, University of Virginia, Charlottesville, VA 22908, USA
3 UVA Brain Institute, University of Virginia, Charlottesville, VA 22908, USA

Correspondence to: Jaideep Kapur MD, PhD
UVA Brain Institute, University of Virginia, Health Sciences Center
PO Box: 801330, Charlottesville, VA 22908, USA
E-mail: jk8t@virginia.edu

Keywords: seizures; epilepsy; TRAP; basal ganglia; striatum; indirect pathway

Abbreviations: aCSF = artificial cerebrospinal fluid; AAV = adeno-associated virus; GFP = green fluorescent protein; GPe = globus pallidus externus; GPi = globus pallidus internus; LFP = local field potential; PV = parvalbumin; SNR = substantia nigra pars reticulata; STN = subthalamic nucleus; TRAP = targeted recombination in active populations; VL = ventrolateral thalamic nucleus; VM = ventromedial thalamic nucleus

Introduction

Epilepsy is a disease that afflicts more than 65 million people worldwide. Frontal lobe epilepsy is the second most common type of epilepsy after temporal lobe epilepsy. However, the neuronal circuits mediating frontal lobe seizures remain poorly understood. Focal motor to bilateral tonic-clonic seizures, previously known as secondarily generalized or partial-onset grand mal, activate the motor cortex.[1] The striatum and its projections to the globus pallidus, subthalamic nucleus, and substantia nigra pars reticulata comprise the basal ganglia and are critical output structures of the motor cortex.[2] Previous studies indicated that basal ganglia

Received July 26, 2020. Revised December 12, 2020. Accepted January 4, 2021. Advance access publication March 17, 2021

participate in seizures.[3–5] However, these studies focused on individual structures, such as the striatum or substantia nigra, and lacked cellular resolution.[6–9]

There are two types of medium spiny neurons interspersed through the striatum. Neurons that express dopamine receptors D2 (DRD2) on their surface comprise the indirect pathway and project to the globus pallidus externus (GPe), subthalamic nucleus (STN), and substantia nigra pars reticulata (SNR), inhibiting voluntary movement. Neurons that express dopamine receptors D1 (DRD1) comprise the direct pathway and project to the globus pallidus internus (GPi) and SNR, facilitating voluntary movement.[10,11] Older studies described modulation of seizures by dopaminergic drugs,[12] but it is unknown whether motor seizures activate the indirect or direct pathway through the striatum. We demonstrate that frontal lobe seizures preferentially activate the indirect pathway neurons of the basal ganglia, predominantly activating DRD2 neurons.

Here, we incorporated novel tools and techniques, such as super-resolution and light-sheet microscopy, activity reporter targeted recombination in active populations (TRAP2) mice, tissue clearing, Cre-driven viral tracing, and local field potential (LFP) recordings from multiple structures simultaneously to map the neuronal activation circuit after frontal lobe focal motor to bilateral tonic-clonic seizures. Additionally, we suppressed seizures by infusing D2 agonists into the striatum, showing that the basal ganglia and D2 system modulate seizures.

Materials and methods

Animals

All studies were approved by the University of Virginia Animal Care and Use Committee. Mice expressing Cre-ER under the regulation of c-Fos promoter (Fos^{CreER}, Jackson Laboratories, #021882, or $Fos^{2A\text{-}ICreERT2}$, Jackson Laboratories, #030323) were crossed to mice expressing tdTomato from the Rosa locus (Ai9, Jackson Laboratories, #007909) to generate TRAP2 mice. TRAP2 and C57BL/6 (Charles River) mice of both sexes (7–12 weeks) were maintained on 12-h light (6 a.m. to 6 p.m.)/dark (6 p.m. to 6 a.m.) cycle and had *ad libitum* access to food and water. For genotyping, KAPA Biosystems kit was used.

Seizure induction, EEG/LFP recordings and virus injections

To induce seizures, TRAP2 or C57BL/6 mice were anaesthetized with isoflurane, a small craniotomy was made, cobalt wire (diameter 0.5 mm, length 1 mm, 1.7 mg) was implanted in the right premotor cortex (AP +2.6 mm, ML –1.8 mm) with four subdural EEG electrodes and a reference (Fig. 1D). Animals were continuously monitored for seizures via video/EEG. All mice developed seizures within 13–20 h after cobalt insertion, and 4-hydroxytamoxifen (4-OHT, 50 mg/kg, s.c.) was injected at the peak of seizures within 90 min. Animals were perfused 5 days after 4-OHT injection to allow tdTomato expression.

Steel wire was used as a control (diameter 0.5 mm, 1.7 mg) and implanted instead of cobalt as described above. 4-OHT was injected 18 h after steel wire implantation (the average time period of seizure peak in cobalt implanted mice). Mice were monitored via continuous video/EEG for 48 h; no seizures were observed.

LFPs were recorded with a custom-made array of microelectrodes (diameter 50 μm, diamel-coated nickel-chromium wire) (Johnson Matthey Inc.). Electrode length of 2 cm maintained 60–70 kΩ resistance. The data were amplified and filtered (the low cut pass 1 Hz, high cut pass 5 kHz) by 16-Channel Microelectrodes Amplifier Model 3600 (A-M Systems), digitized, and stored on a computer with PowerLab 16/35 hardware and LabChart 8 software at a sampling rate of 10 kHz. We coordinated the distance between each microelectrode's array by using non-epileptic animals with the cross-correlation to be <0.7 between each electrode, by analysing the time lag between the electrodes (in MATLAB). The cross-correlation r and delay d are defined as:

$$r = \frac{\sum_i [(x(i) - mx) * (y(i-d) - my)]}{\sqrt{\sum_i (x(i) - mx)^2} \sqrt{\sum_i (y(i-d) - my)^2}} \quad (1)$$

where $x(i)$ and $y(i)$ are two series with $i = 0, 1, 2 \ldots N-1$, and mx and my are the means of the corresponding series. To record seizures, the microelectrodes were placed in the premotor cortex (AP +2.2 mm, ML –1.8 mm, DV –0.5 mm), striatum (AP +1.2 mm, ML –1.8 mm, DV –3.5 mm), ventrolateral thalamic nucleus (VL) (AP –1.3 mm, ML –1.0 mm, DV –3.75 mm), and SNR (AP –3.3 mm, ML –1.5 mm, DV –4.75 mm) together with cobalt. Seizure start was identified as a deflection of the voltage trace at least twice the baseline after visual inspection. After recordings, the electrode position was marked by applying a single burst of 40 μA, 0.75 ms monophasic square wave pulse at 50 Hz for 30 s using a constant current stimulator (A-M Systems, Model 2100). The animals were perfused, brains were sectioned 40-μm thick on a cryostat (Leica, CM1900), and stained with DAPI [0.02% in phosphate-buffered saline (PBS)]. The sections were imaged on Nikon Eclipse Ti-S, 2×/0.45 NA. If the electrode position was incorrect, the data were excluded from the analysis.

LabChart LFP data were analysed to create spectrograms, using Fast Fourier Transform with a Cosine-Bell data window and a window size of 1024 data-points (2.56 s), which resulted in a frequency resolution of 0.375 Hz. A window overlap of 87.5% was used to smooth the spectrogram's x-axis. We expressed power as μV^2.

TRAP2 mice were injected with either AAV9-CamKII0.4.eGFP.WPRE.rBG (#105541-AAV9, Addgene) or AAV9 pCAG-FLEX-EGFP-WPRE (#51502-AAV9, Addgene) in the premotor cortex (AP +2.6 mm, ML –1.8 mm, DV –0.5 mm; 100 nl) with Hamilton syringe (#7634-01). A minimum of 2 weeks was allowed for the viral expression before proceeding with cobalt implantation.

Immunohistochemistry

Mice were deeply anaesthetized with isoflurane and perfused intracardially with 4% paraformaldehyde (PFA) in 0.1 M phosphate buffer, pH 7.2 at 4°C. Brains were fixed in PFA overnight, cryoprotected in 30% sucrose in PBS for 2 days at 4°C, and sliced on a cryostat at 40 μm. Each fourth section was placed in a blocking buffer [50 μl/ml normal goat serum (NGS), #017-000-121, Jackson ImmunoResearch, and 0.1% Triton™ X-100] for 2 h. The primary antibodies (with 20 μl/ml NGS overnight at 4°C) were rabbit anti-D2R (1:250, #AB5084P, Millipore), rat anti-D1R (1:300, #D2944, Sigma), rabbit anti-NeuN (1:250, #24307, Cell Signaling), rabbit anti-GFAP (1:800, #ab7260, Abcam), mouse anti-MBP (1:500, #ab62631, Abcam), rabbit anti-enkephalin (1:2000, #20065, ImmunoStar), guinea pig anti-dynorphin (1:500, #AB5519, Millipore), rabbit anti-PV (1:500, #ab11427, Abcam), and rabbit anti-preproenkephalin (1:1000, #RA14124, Neuromics). The sections were washed in 1× PBS. The secondary antibodies (1:500, Invitrogen, for 2 h at room temperature) were 405 goat anti-rabbit, 488 goat anti-rabbit, 488

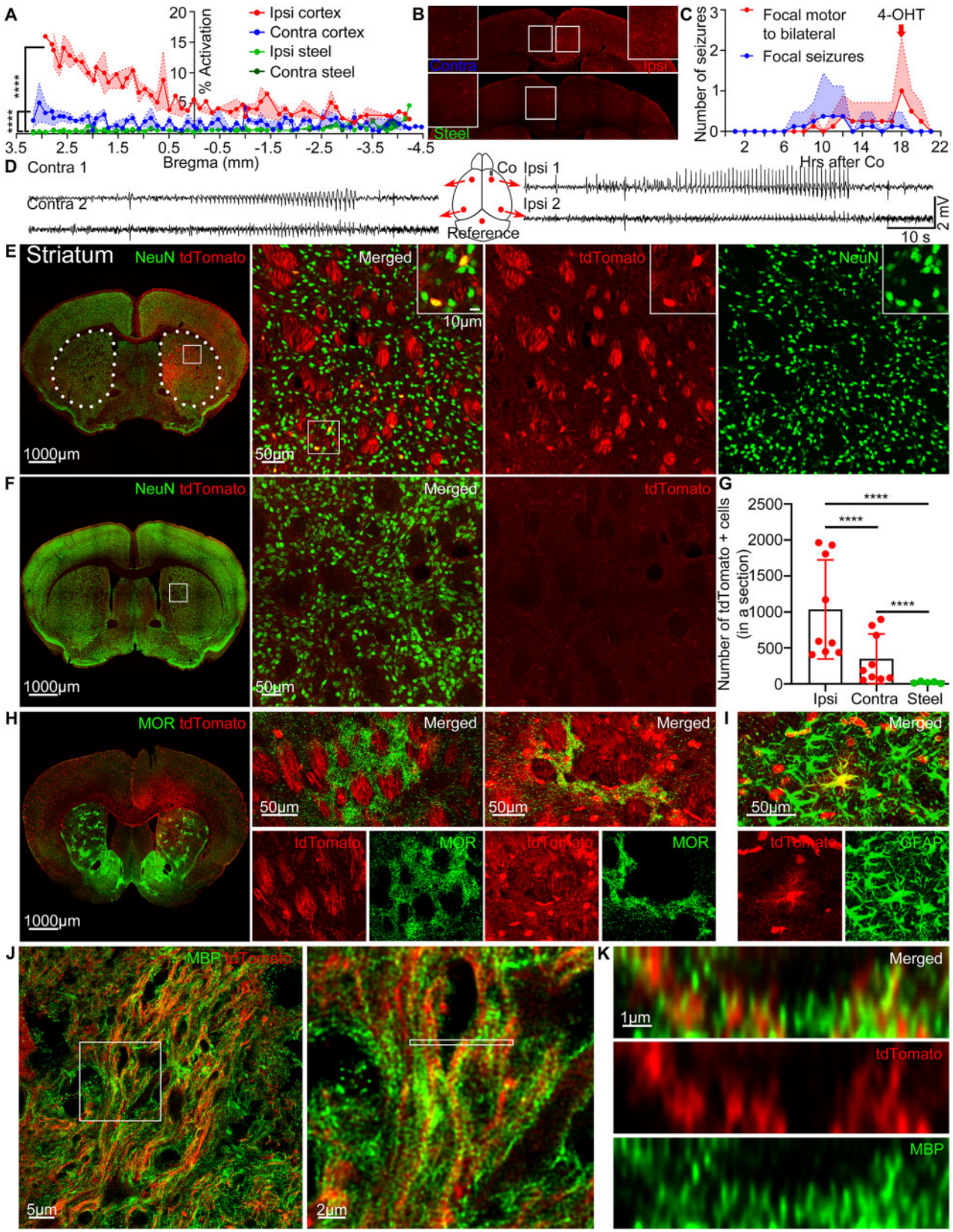

Figure 1 Frontal lobe seizures activate the striatum. (**A**) % Activation in the ipsilateral (red) and contralateral (blue) cortex in mice with seizures compared to the ipsilateral (green) and contralateral (dark green) cortex of the control steel wire implanted mice without seizures across the whole brain from the anterior (3.5 mm bregma) to the posterior cortex (–4.5 mm bregma), Kolmogorov-Smirnov test, n = 4–6 mice. (**B**) Representative tdTomato expression in the ipsilateral (red) and contralateral (blue) cortex in mice with seizures compared to the steel wire control mice without seizures (green), quantification in **A**. *Boxed insets*: Enlarged images from the middle areas. (**C**) After cobalt implantation, TRAP mice developed spontaneous repeated focal seizures (blue) and focal motor to bilateral tonic-clonic seizures (red). 4-OHT was injected at the peak of secondarily

(continued)

goat anti-guinea pig, 488 goat anti-mouse, 488 goat anti-rat, and 633 goat anti-rat.

Processing, image acquisition, drug treatment and analysis

Mice were perfused with 4% PFA and 4% acrylamide in 0.1 M phosphate buffer to clarify tissue. Brains were fixed in the same solution overnight at 4°C. Sections (200 μm thick) were sliced on a vibratome (Leica VT3200) and incubated in 1% acrylamide in PBS with 0.25% VA-044 (#27776-21-2, Wako Chemicals) in the dark overnight at 4°C. The sections were degassed in nitrogen for 1–5 min, polymerized at 37°C for 3 h, washed in PBS, and incubated with 8% sodium dodecyl sulphate (SDS, Bio-Rad) in PBS at 37°C for 24–36 h covered in parafilm until transparent. For whole-brain clearing, SDS was changed every day for 2 weeks until the whole brain became transparent. The sections were then washed in PBS with 0.1% Triton™ X-100 and mounted in RIMS (40 g Histodenz™ in 30 ml 0.2 M phosphate buffer, 0.1% Tween-20, 0.01% sodium azide, pH 7.5).

Confocal images were done on Nikon Eclipse Ti-U at 10×/0.45 NA or 20×/0.95 NA, 1024 × 1024 frame size. Images were tiled as stacks with 5 μm z-interval and stitched using NIS-Elements software. Imaris 9.3.0 (Bitplane) was used for visualization and Adobe Photoshop CC for cropping an original image and figure display. DRD2 or DRD1 were imaged on Zeiss LSM 980 Multiphoton Airyscan 2 at 63×/1.40 NA, oil, or Leica SP8 STED at 93×/1.30 NA, glycerol. One-third of the whole clarified brain was imaged on Zeiss Z.1 Light Sheet microscope with objective lens 5×/0.1 NA, detection objective lens 5×/0.16 NA, and arivis Vision4D software. Excitation lasers were 405, 488, 561 and 633 nm.

For sumanirole versus artificial CSF (aCSF) treatment, C57BL/6 mice were implanted with cobalt, four surface EEG electrodes, a reference, and a bilateral guide cannula (PlasticsOne, C235G-2.7/SPC, 26 GA, 2.1 mm below pedestal) at AP +1.02 mm, ML ±1.35 mm, DV –1.75 mm into the striatum and stabilized with dental cement. An internal bilateral cannula (PlasticsOne, C235I/SPC, 33GA, 1 mm projection) was connected to two 5 μl Hamilton syringes prefilled with either sumanirole maleate (10 μg/injection per lobe in aCSF) or aCSF (in mM, 127 NaCl, 2 KCl, 1.5 $MgSO_4$, 25.7 $NaHCO_3$, 10 dextrose, and 1.5 $CaCl_2$; 300 mOsm) as a control, and injected by a blinded experimenter slowly over 75 s at 18 h after cobalt insertion. The blinded experimenter counted seizures before the injections (15–18 h after cobalt) to determine the baseline, following the injections (18–20.5 h after cobalt) because sumanirole has a sustained effect for at least 2 h, and after the injections (20.5–23.5 h after cobalt) to determine return to the baseline.

To count the number of tdTomato-positive cells in cobalt versus steel implanted mice, Imaris Spots detection or ImageJ were used and confirmed manually by a blinded investigator. A region of interest was drawn, background was subtracted, and the threshold was adjusted. The number of cells was counted on a 40 μm cryostat section in a structure and averaged across sequential sections in a mouse. Each point on a graph is the average value for a separate mouse. At least three sections were analysed per lobe per animal. In the steel wire implanted mice, left and right lobe data were combined and averaged in each animal.

To determine whether DRD2/DRD1- or ENK/DYN-positive cells co-localized with tdTomato-positive cells, tdTomato cells were tagged using Imaris Spots detection tool on ×20 confocal images. Co-localization was manually checked based on whether ∼50% of the surface co-localized with the marker of interest. The number of tdTomato-positive cells that co-localized with either DRD2 or DRD1 (ENK or DYN) was divided by the total number of all tdTomato-positive cells, which allowed us to determine per cent of tdTomato cells expressing the marker.

Statistics

All statistical analysis was performed in Prism 8. Unpaired t-test was used for normally distributed and the Kolmogorov-Smirnov test for data not normally distributed. Data are presented as mean ± standard error of the mean (SEM), where n is the number of animals or the number of seizures followed by the number of animals. Results were considered statistically significant for $P < 0.05$.

Data availability

The data that support the findings are available from the corresponding authors upon request.

Results

Frontal lobe seizures activate the striatum

To visualize neuronal activation during seizures, we used TRAP mice, modified to a new generation TRAP2 that utilizes the activity of immediate early gene c-Fos to drive Cre expression.[13,14] 4-OHT injection translocates Cre inside the nucleus that relieves the repression from tdTomato, which labels activated cells. Non-active cells are not labelled with tdTomato because they do not express Cre. To initiate frontal lobe focal motor to bilateral tonic-clonic seizures, we used a well-characterized cobalt model.[15–18] Cobalt inactivates oxygen-binding molecules within neurons, causing hypoxic injury.[19] Cobalt wire (1.7 mg) was inserted into the right premotor cortex of a TRAP mouse with five subdural EEG electrodes on both hemispheres (Fig. 1D). The mice were monitored for seizures via continuous video/EEG. Interictal spike-wave

Figure 1 Continued
generalized tonic-clonic seizures within 90 min of the last seizure (red arrow). Points indicate mean and shaded regions SEM (n = 8 mice). (**D**) A schematic of the cobalt placement and EEG electrodes (red), and a representative EEG recording from each electrode during focal motor to bilateral seizure in a TRAP mouse. (**E**) *Left*: tdTomato (red) expression in the striatum immunolabelled for NeuN (green). Dotted lines indicate the striatum. *Right*: Magnified view of the striatum. *Boxed inset*: tdTomato-positive neurons co-localized with NeuN. (**F**) *Left*: Steel wire control showed minimal tdTomato expression in the striatum. *Right*: Magnified view of the striatum. (**G**) Cobalt implanted mice had more tdTomato-positive cells in the ipsilateral and contralateral striatum compared to the steel wire implanted mice (each point is the average number of cells in a 40 μm section across sequential striatal sections in a mouse) (ipsilateral: 1036 ± 229.4 cells, n = 9 mice, Kolmogorov-Smirnov test; contralateral: 349.8 ± 115.2 cells, n = 9 mice, Kolmogorov-Smirnov test; control: 20.90 ± 5.909 cells, n = 5 mice). The ipsilateral striatum had more tdTomato-positive cells than the contralateral in mice with seizures (Kolmogorov-Smirnov test). (**H**) *Left*: Striosomes immunolabelled for MOR (green) and tdTomato expression in the striatum. *Middle*: Striosome that did not express tdTomato. *Right*: Striosome that was tdTomato positive. (**I**) An astrocyte immunolabelled for GFAP (green) expressed tdTomato in the striatum. (**J**) *Left*: SP8 super-resolution lightning microscopy image of tdTomato-positive myelinated axons immunolabelled for myelin basic protein (MBP) (green) in the ipsilateral striatum. *Right*: Magnified view of myelinated tdTomato-positive axons. (**K**) Cross-section of myelinated axons containing tdTomato indicated by the thin white rectangle in **J**. Data are mean ± SEM, (Kolmogorov-Smirnov test), ****$P <$ 0.0001. Also, see Supplementary Video 1.

discharges appeared in the EEG within hours after recovery from surgery and became more frequent and bilateral. Spontaneous focal and focal to bilateral tonic-clonic seizures repeatedly occurred over the next 6–36 h and lasted 10–180 s (Fig. 1C). Animals were injected with 4-OHT (50 mg/kg, s.c.) 90 min after focal to bilateral seizures to cause recombinant expression of tdTomato in activated neurons. In a separate experiment, we found that tdTomato expression peaks when 4-OHT is administered 90 min following a seizure. This time course is consistent with c-Fos mRNA expression after a seizure.[20–23] After 5 days of tdTomato protein accumulation, the whole brain was serially sectioned into 40 μm sections and imaged on a confocal microscope to analyse the pattern of tdTomato expression.

Secondarily generalized tonic-clonic seizures led to cortical activation in both hemispheres, as seen on bilateral EEG (Fig. 1D) and in increased tdTomato signal (Fig. 1A and B). The ipsilateral hemisphere of mice with seizures had more tdTomato signal than the contralateral (Fig. 1A and B), where % activation is the total tdTomato fluorescence in the cortex divided by the total cortical area. Observed cortical activation could be a result of motor activity, cortical injury, or seizures. We implanted steel wire instead of cobalt and injected 4-OHT 18 h after the surgery. The control steel wire mice had no seizures and showed minimal cortical tdTomato expression (Fig. 1A and B).

The dorsal striatum strongly expressed tdTomato (Fig. 1E). The ipsilateral striatum to the seizure focus expressed more tdTomato-positive cells than contralateral (Fig. 1E and G). The graph (Fig. 1G) represents the average number of tdTomato-positive cells on a 40 μm section across sequential striatal sections in a mouse, where each point is the average value for a separate mouse. The striatum of the control mice had fewer tdTomato-positive cells compared to both the ipsilateral and contralateral striatum of the mice with seizures (Fig. 1F and G). tdTomato was observed throughout the whole striatum from the anterior to the posterior sections. Neurons in the striatum expressed tdTomato; however, not all neuronal somas were tdTomato positive. We will demonstrate below the electrographic activation of the striatum, which is the result of the neuronal firing. Striatal bundles also expressed tdTomato (Fig. 1E). Myelinated axon fibres course through the striatum, and our previous studies have suggested that tdTomato can fill axons. We tested whether the fibre bundles were myelinated axons filled with tdTomato, using an antibody against myelin basic protein (MBP) (Fig. 1J). SP8 super-resolution lightning microscopy revealed myelin spiralling and wrapping around the tdTomato expressing axons (Fig. 1J and Supplementary Video 1). The cross-sectional view demonstrated that myelin surrounded each axon containing tdTomato (Fig. 1K). Additionally, the striatum is made up of the striosomes (also called patches), which express μ-opioid receptors (MOR), and the surrounding matrix.[24] Both limbic and sensorimotor cortical areas project to the striosomes and matrix, but the striosomes receive more inputs from limbic cortical regions.[25] The striosomes did not express tdTomato (Fig. 1H). Only rare occasional striosomes close to the midline were tdTomato positive (Fig. 1H). We also found a few tdTomato-positive cells that did not co-localize with NeuN. Astrocytes are known to play a role in ictogenesis.[26] To visualize astrocytes, we used the anti-GFAP antibody and found few astrocytes that expressed tdTomato (Fig. 1I).

Seizures activate the indirect basal ganglia pathway neurons

We conducted a series of experiments to investigate whether focal motor to bilateral tonic-clonic seizures activate the indirect (dopamine receptor D2-expressing) or direct (dopamine receptor D1-expressing) pathway. D2 agonists exert anticonvulsant action and suppress pilocarpine and kindled seizures,[12,27] whereas D1 agonists and D2 antagonists are pro-convulsant.[28] Patients taking high-affinity D2 antagonists for schizophrenia or psychosis have a higher risk of seizures.[29–32] However, these studies demonstrate D2 receptor modulation of seizures and do not report activation of the striatum or activation of the medium spiny neurons during seizures.

We used a highly selective full D2 agonist, sumanirole, to determine if modulation of the indirect pathway would be protective against cobalt-induced seizures. Sumanirole has more than 200-fold selectivity for the D2 receptors over other dopamine receptor subtypes and a sustained effect for at least 2 h with onset starting around 30 min post-injection in rodents.[33–37] Because dopamine receptors D2 are also highly expressed in the cortex in addition to the medium spiny neurons of the indirect pathway, we injected sumanirole directly into the anterior striatum via a bilateral cannula. After implanting C57BL/6 mice with cobalt, they received one blinded injection of either sumanirole (10 μg/injection per lobe in aCSF) or aCSF 18 h after cobalt insertion via a bilateral cannula and were monitored via video/EEG for another 10 h (Fig. 2A and D). After the injection, both groups of mice did not have a noticeable behavioural or electrographic change and continued having spike-wave discharges after cobalt insertion (Fig. 2B). None of the sumanirole-injected mice experienced seizures during 2.5 h following the injection as determined by a blinded investigator, whereas the aCSF-injected mice had more seizures (Fig. 2C), which indicates that the D2 receptor agonist is anticonvulsant in cobalt-induced seizures.

It is unknown whether seizures activate the indirect or direct pathway. We wanted to quantitatively assess whether the tdTomato-positive medium spiny neurons expressed either D2 or D1 receptors in the striatum. The entire striatum of TRAP mice after a seizure was serially sectioned and immunolabelled for D2 and D1 receptors (Fig. 2E and F).[38] Around 80% of all activated neurons in the striatum expressed DRD2 in the ipsilateral and contralateral striatum and not DRD1 (Fig. 2I). The proportion of activated DRD2- versus DRD1-positive neurons remained constant throughout the striatum from the anterior to posterior sections, suggesting no rostrocaudal gradient (Fig. 2J).

We performed confirmatory experiments by immunolabelling for enkephalin and dynorphin (Fig. 2G and H). The majority of indirect pathway neurons express enkephalin (ENK), whereas the majority of the direct pathway medium spiny neurons express substance P and dynorphin (DYN).[39,40] Similarly, around 80% of all activated neurons in the striatum expressed ENK and not DYN, which indicates preferential activation of the indirect pathway neurons (Fig. 2K).

Dopamine receptors are expressed on the neuronal membrane, and tdTomato expression is intracellular.[41] False positives are possible due to other labelled cells lying on top within a 40 μm section. To counter this problem, we carried out SP8 super-resolution STED (stimulated emission depletion) microscopy imaging of triple labelled sections with anti-DRD2 and anti-DRD1 antibodies. Super-resolution microscopy confirmed that tdTomato-positive cells express DRD2 and not DRD1 (Fig. 3). We also found examples of membranous, nuclear and cytoplasmic expression of DRD2 (Fig. 3A–C).

Activation of the GPe, STN and SNR in addition to the thalamus

Next, we investigated the activity of the striatal projection targets. The indirect pathway D2 medium spiny neurons project to the GPe, STN, and SNR, whereas the direct pathway D1 medium spiny

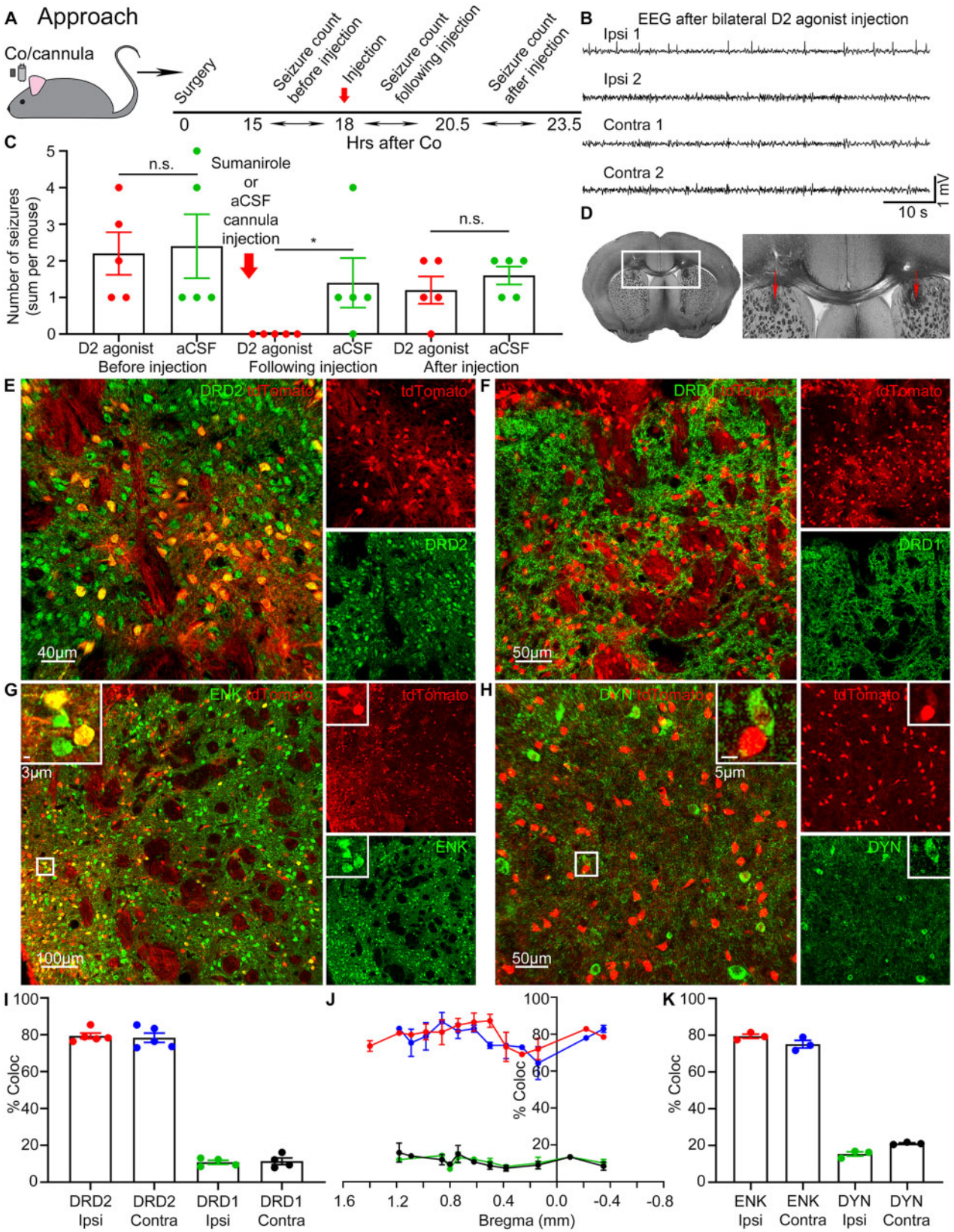

Figure 2 Seizures activate the indirect basal ganglia pathway neurons. (**A**) C57BL/6 mice were implanted with cobalt and a bilateral cannula. Sumanirole or aCSF was injected via a bilateral cannula into the striatum at 18 h after cobalt (red arrow). The number of seizures was counted by a blinded experimenter before the injection (15–18 h after cobalt), following (18–20.5 h after cobalt), and after the injection (20.5–23.5 h after cobalt). (**B**) A representative EEG 20 min after bilateral sumanirole injection into the striatum. (**C**) The effect of either sumanirole (red) or aCSF (green) injection (red arrow) on the number of seizures before the injection (15–18 h after cobalt) (sum per mouse, n = 5 mice): D2 agonist: 2.2 ± 0.58, aCSF: 2.4 ± 0.87 (Kolmogorov-Smirnov test), following the injection (18–20.5 h after cobalt): D2 agonist: 0.0 ± 0.0, aCSF: 1.4 ± 0.68 (P = 0.0476, Kolmogorov-Smirnov

(continued)

neurons project to the GPi and SNR. The direct and indirect pathways are segregated.[11,40,42–50]

The Paxinos Brain Atlas does not distinguish between the external and internal segments of the globus pallidus in a mouse brain.[51] Therefore, we adopted the online Allen Brain Reference Atlas distinction between GPe and GPi, which shows the GPe located medial to the posterior striatum and lateral to the septum and internal capsule. The GPi is posterior relative to the GPe, where the hippocampus first appears, medial to the GPe and lateral to the reticular thalamic nucleus and internal capsule. Parvalbumin (PV) immunolabelling allowed easy visualization of the location of the reticular thalamic nucleus and GPe (up to 59% of all GPe neurons express PV).[52–55]

The GPe, a part of the indirect pathway, strongly expressed tdTomato (Fig. 4A and C). Neurons expressed tdTomato in the ipsilateral GPe to the seizure focus, which had more tdTomato-positive cells than the contralateral (Fig. 4A and E). The GPe of the control mice had fewer tdTomato-positive cells compared to both the ipsilateral and contralateral GPe of the mice with seizures (Fig. 4D and E). Not only neurons but also axonal fibres in the GPe were tdTomato positive (Fig. 4A and C). There are two types of GPe neurons, prototypic (PV positive that project to the STN) and arkypallidal (FoxP2 and preproenkephalin positive that project to the striatum).[56] Prototypic cells inhibit arkypallidal, and the STN is reciprocally connected and provides excitatory input to both cell types. We found that almost none of the PV neurons in the GPe expressed tdTomato (Fig. 4C), suggesting that seizures do not activate prototypic GPe cells. We immunolabelled GPe for arkypallidal neurons with anti-preproenkephalin antibody and found that almost all of the tdTomato cells in GPe were arkypallidal (Fig. 4B). It was recently reported that activation of the indirect (D2) medium spiny neurons inhibits prototypic cells, disinhibiting the STN and arkypallidal cells.[56] However, it is possible that GPe arkypallidal neurons were activated directly from the cortex.

The GPi, a part of the direct pathway, had similar tdTomato expression as the background activity of the controls (Fig. 4F–H). Both the ipsilateral and contralateral GPi in mice with seizures had a similar number of tdTomato-expressing cells as the GPi of the controls. The number of tdTomato-positive cells was also similar in the ipsilateral and contralateral GPi.

The STN strongly expressed tdTomato in both hemispheres (Fig. 5A). The STN is a lens-shaped nucleus that lies below the posterior and ventrobasal thalamic nuclei above the cerebral peduncle and receives GABAergic projections from the GPe as a part of the indirect pathway. Both the ipsilateral and contralateral STN of mice with focal motor to bilateral tonic-clonic seizures had more tdTomato-expressing cells than the STN of the controls (Fig. 5B and C). The number of tdTomato-positive cells in the ipsilateral STN was similar to that in the contralateral STN (Fig. 5C).

The SNR also expressed tdTomato (Fig. 5D). Located laterally to the mammillary nuclei, SNR receives GABAergic projections from the striatum via the direct pathway and glutamatergic projections from the STN via the indirect pathway, while sending GABAergic projections to the motor thalamic nuclei such as the ventrolateral and ventromedial.[57] Both the ipsilateral and contralateral SNR had more tdTomato-expressing neurons than the SNR of the controls (Fig. 5D–F). The ipsilateral SNR had more tdTomato-expressing cells than the contralateral (Fig. 5F).

Motor thalamic nuclei also expressed tdTomato (Fig. 6A). The motor thalamus consists of the ventroanterior/ventrolateral (VA/VL) and ventromedial (VM) nuclei. These nuclei receive reciprocal projections from the motor cortex and GABAergic inhibitory projections from the SNR.[57,58] Motor thalamic nuclei VL/VM ipsilateral to the seizure focus were active and expressed more tdTomato-positive cells than the contralateral or VL/VM of the control mice without seizures (Fig. 6A–D). Ipsilateral centromedian,[59] mediodorsal, and anterior reticular thalamic (RTN) nuclei were tdTomato positive as well (Figs 4F and 6A, E and F).

Electrographic activation of the basal ganglia during seizures

The TRAP technique has limited temporal resolution, so we recorded LFP from the premotor cortex, motor thalamic nucleus VL, striatum, and SNR simultaneously. We selected the VL because of its larger size compared to other motor thalamic nuclei and, thus, easier electrode targeting. Custom-made array of microelectrodes recorded LFPs at a 10 kHz sampling rate, which allowed us to detect seizure spread with millisecond precision (Fig. 7A). To establish that the source of electrical activity recorded from one microelectrode was independent of that from a neighbouring microelectrode, we analysed the cross-correlation of activities recorded from two neighbouring electrodes. The cross-correlation has to be <0.7 for the activities to be considered independent. Microelectrodes with 60–75 kΩ resistance and 2 cm length yielded recording without significant cross-contamination (<0.7) (Fig. 7B). The location of the electrodes was marked by applying a single burst of 40 μA, 0.75 ms monophasic square wave pulse at 50 Hz for 30 s after the recordings were complete. The data were analysed only if the electrode tip location was correct (Fig. 7C).

Simultaneous LFP recordings from the premotor cortex, VL, striatum, and SNR ipsilateral to the seizure focus confirmed that focal motor to bilateral tonic-clonic seizures indeed activate these structures (Fig. 7D). Seizures, consisting of rhythmic spike-wave discharges mixed with low amplitude fast (gamma) activity, were recorded from each of these structures. Next, we compared seizure onset time in each structure to the onset time at the seizure focus in the premotor cortex. Surprisingly, some seizures required several hundred milliseconds to arrive at the striatum or SNR; in contrast, other seizures took several seconds to appear in these structures, suggesting two populations based on latency, fast (<200 ms) and slow (>200 ms). In recordings from the striatum, 70% of seizures were short latency, and the rest took longer (Fig. 7F). In the SNR, similarly, 48% of seizures were short latency, and the remaining seizures had longer latency (Fig. 7G). However, all of the seizures required <200 ms to arrive at the VL (Fig. 7E). We

Figure 2 Continued

test), and after the injection (20.5–25.5 h after cobalt): D2 agonist: 2.2 ± 0.37, aCSF: 2.0 ± 0.45 (unpaired *t*-test). (**D**) Light microscope image of the traces left from the bilateral cannula targeting dorsal anterior striatum (red arrows). (**E**) DRD2 (green) and tdTomato (red) expression in the striatum. (**F**) DRD1 (green) and tdTomato expression in the striatum. (**G**) ENK (green) and tdTomato expression in the striatum. *Boxed inset:* tdTomato-positive neurons co-localized with ENK. (**H**) DYN (green) and tdTomato expression in the striatum. *Boxed inset*: The majority of tdTomato-positive neurons did not co-localize with DYN. (**I**) % Co-localization of tdTomato-positive cells with either DRD2 or DRD1 in the striatum. Co-localization of tdTomato with: DRD2 in the ipsilateral striatum (red): 79.71 ± 1.857%; DRD2 in the contralateral striatum (blue): 78.40 ± 2.542%; DRD1 in the ipsilateral striatum (green): 10.93 ± 1.085%; DRD1 in the contralateral striatum (black): 11.55 ± 1.736%, (n = 4–5 mice). (**J**) Point line graph of the data in (**I**) across bregma from the anterior (1.6 mm) to posterior (–0.8 mm) striatum. (**K**) % Co-localization of tdTomato-positive cells with either ENK or DYN in the striatum. Co-localization of tdTomato with: ENK in the ipsilateral striatum (red): 79.46 ± 1.158%; ENK in the contralateral striatum (blue): 75.09 ± 2.092%; DYN in the ipsilateral striatum (green): 15.43 ± 1.170%; DYN in the contralateral striatum (black): 21.12 ± 0.3507%, (n = 3 mice). Data are mean ± SEM, Kolmogorov-Smirnov test, n.s. = non-significant. *$P <$ 0.05.

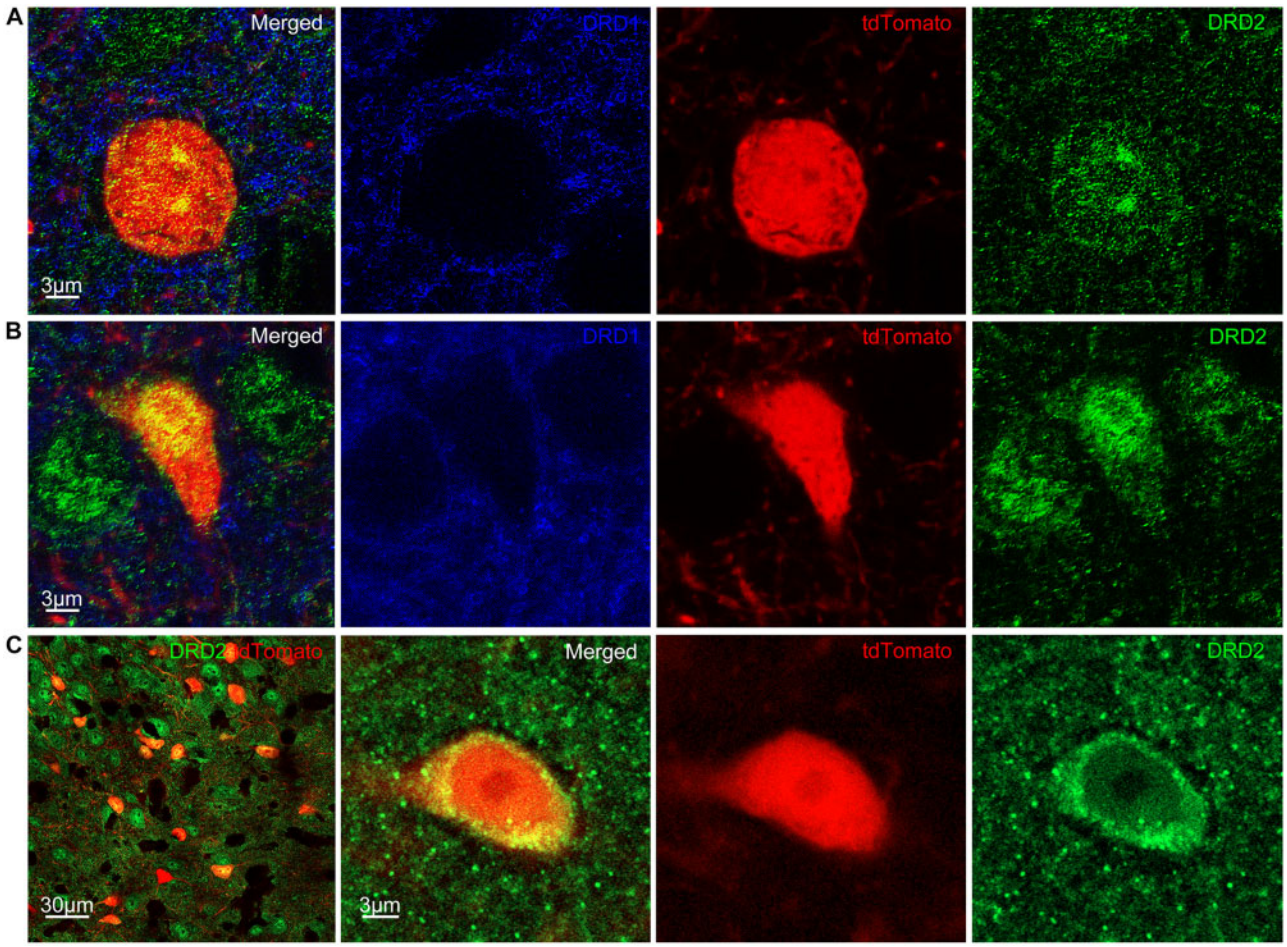

Figure 3 Activated cells in the striatum express DRD2 but not DRD1. (**A**) SP8 super-resolution STED image shows tdTomato-positive cells (red) express DRD2 (green) but not DRD1 (blue) on the neuronal membrane in the striatum. (**B**) STED image shows tdTomato-positive cells express DRD2 (green) but not DRD1 (blue) inside the nucleus in the striatum. (**C**) *Left*: LSM 980 Airyscan 2 image shows tdTomato-positive cells express DRD2 (green) in the striatum. *Right*: Magnified view of cytoplasmic DRD2.

found that some seizures required up to ~10 s to appear in the striatum or SNR, which suggests that internal inhibition exists within these structures during some seizures, which prevents immediate ictal onset within them.

We also discovered that after seizure invaded the SNR, spike frequency in the cortex and thalamus decreased by half (Fig. 7H and I). Spike frequency was defined as the number of spikes per second (Fig. 7I). In long latency seizures during onset delay in the SNR, faster cortical and thalamic spikes were detected, whereas after seizure started in the SNR, cortical and thalamic spike frequency dropped (Fig. 7D and H), which could be a delayed hypersynchronized activity in the cortex/thalamus, which is even measurable from the SNR. In short-latency seizures, where seizures started almost simultaneously in the cortex, thalamus, and SNR, no such spike frequency change was noticed, and spike frequency was slower to begin with (Supplementary Fig. 1). Thus, activation of the basal ganglia circuit modulates seizures. In particular, activation of the SNR exerts an inhibitory effect on thalamocortical projections, inhibiting ongoing movement.[60]

Anatomical connections of the seizure focus determine seizure circuit

We hypothesized that anatomical projections of the seizure focus influence seizure propagation, so we tracked both in a single experiment. To trace the efferent connections from the seizure focus, we injected AAV9 GFP virus (AAV9-CamKII0.4.eGFP.WPRE.rBG) in TRAP2 mice at the same coordinates in the premotor cortex 2 weeks before the cobalt insertion surgery. We injected 4-OHT 90 min after focal to bilateral seizures and clarified either anterior one-third of the whole brain and imaged it using a light sheet microscope or clarified 200 μm thick sections, imaged them in tiles, and reconstructed into whole slice images on a confocal microscope.[61]

GFP and tdTomato extensively co-localized in the striatum, indicating that seizures followed anatomical projections from the seizure focus (Fig. 8A). To gain better resolution of the axons expressing both tdTomato and the virus, we used SP8 super-resolution lightening microscopy to image a single axonal bundle from a horizontal section in the striatum. tdTomato-positive axons expressed AAV9-GFP (Fig. 8B and Supplementary Video 2). Thick 200-μm clarified sections revealed how GFP and tdTomato-positive axons traverse from the ipsilateral anterior to posterior striatum (Fig. 8D). Not all tdTomato-positive axons expressed AAV9-GFP because seizures can travel multiple synapses, whereas this Cre-independent virus has not been reported to transport trans-synaptically.[62] Additionally, cortico-cortical spread allowed seizure to reach the striatum from a different cortical location that was not labelled by the virus, and not all of the neurons at the seizure focus could be labelled with AAV9. During focal seizures, LFP recordings

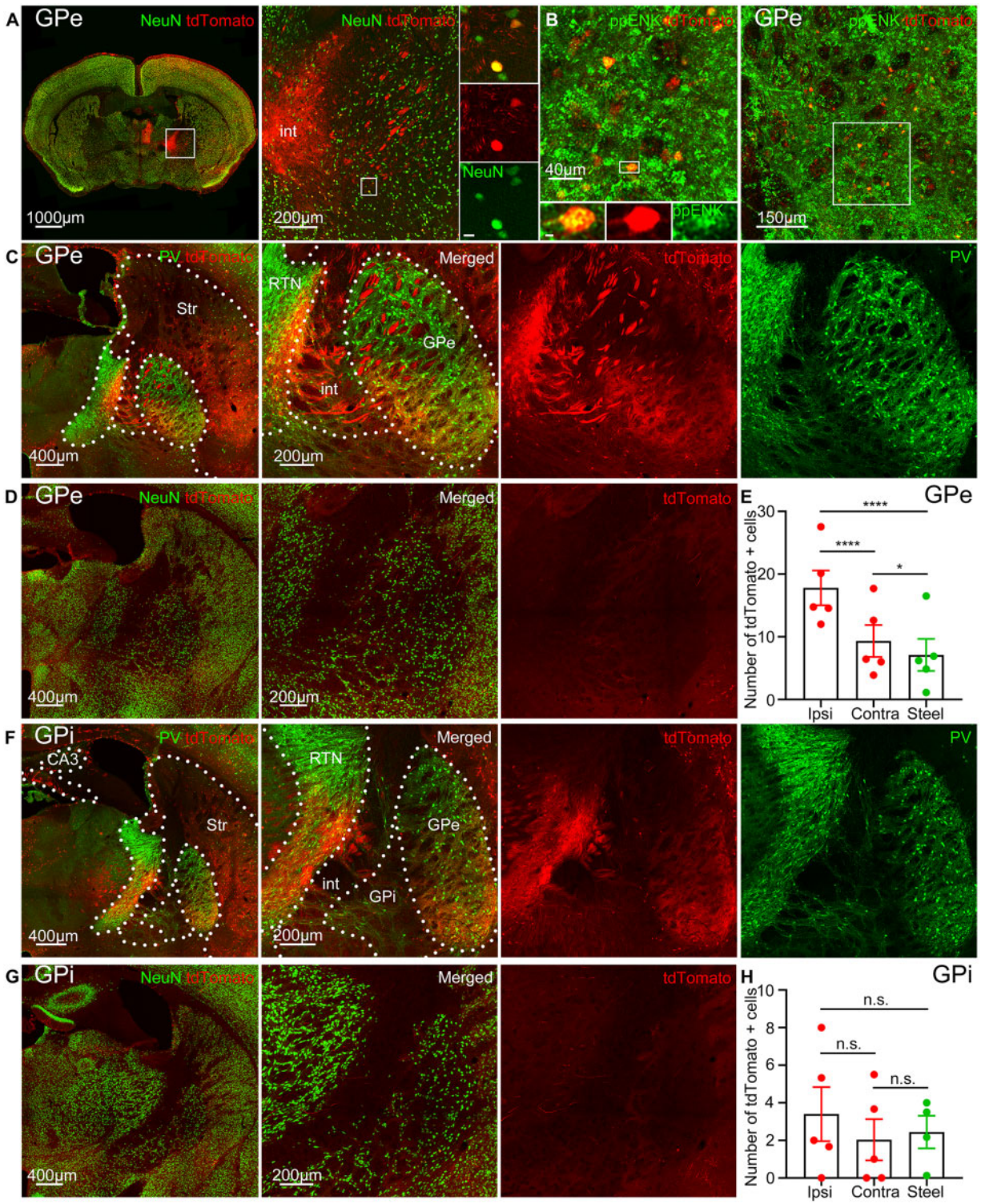

Figure 4 Activation of the GPe of the indirect pathway but not GPi of the direct pathway. (**A**) tdTomato (red) expression in the GPe immunolabelled for NeuN (green) and its magnified view. *Boxed inset*: tdTomato-positive neurons co-localized with NeuN. (**B**) tdTomato expression in arkypallidal GPe neurons immunolabelled for preproenkephalin (ppENK, green). (**C**) tdTomato expression in the GPe immunolabelled for PV, (green) and its magnified view. Dotted lines indicate nuclear boundaries: str = striatum; RTN = reticular thalamic nucleus; int = internal capsule. (**D**) *Left*: Steel wire control showed minimal tdTomato expression in the GPe. *Right*: Magnified view of the GPe. (**E**) Cobalt-implanted mice had more tdTomato-positive cells in both the ipsilateral and contralateral GPe compared to the steel wire implanted mice (each point is the average number of cells in a 40 μm section across sequential GPe sections in a mouse) (ipsilateral: 17.81 ± 2.778 cells, unpaired *t*-test; contralateral: 9.329 ± 2.553 cells, $P = 0.0109$, unpaired *t*-test; control: 7.118 ± 2.550 cells; $n = 5$ mice). The ipsilateral GPe had more tdTomato-positive cells than the contralateral in mice with seizures (unpaired *t*-test). (**F**) *Left*: Minimal tdTomato expression in the GPi during seizures immunolabelled for PV (green). *Right*: Magnified view of the GPi. Dotted lines indicate nuclear boundaries. (**G**) *Left*: Steel wire control showed minimal tdTomato expression in the GPi. *Right*: Magnified view of the GPi. (**H**) Cobalt-implanted mice had similar tdTomato expression in both the ipsilateral and contralateral GPi as the control mice (each point is the average number of cells in a 40 μm section across sequential GPi sections in a mouse) (ipsilateral: 3.400 ± 1.439 cells, unpaired *t*-test; contralateral: 2.033 ± 1.096 cells, unpaired *t*-test; control: 2.448 ± 0.8656 cells; $n = 5$ mice). The number of tdTomato-positive cells in the ipsilateral and contralateral GPi was similar (unpaired *t*-test). Data are mean ± SEM, n.s. = non-significant. $^{*}P < 0.05$, $^{****}P < 0.0001$.

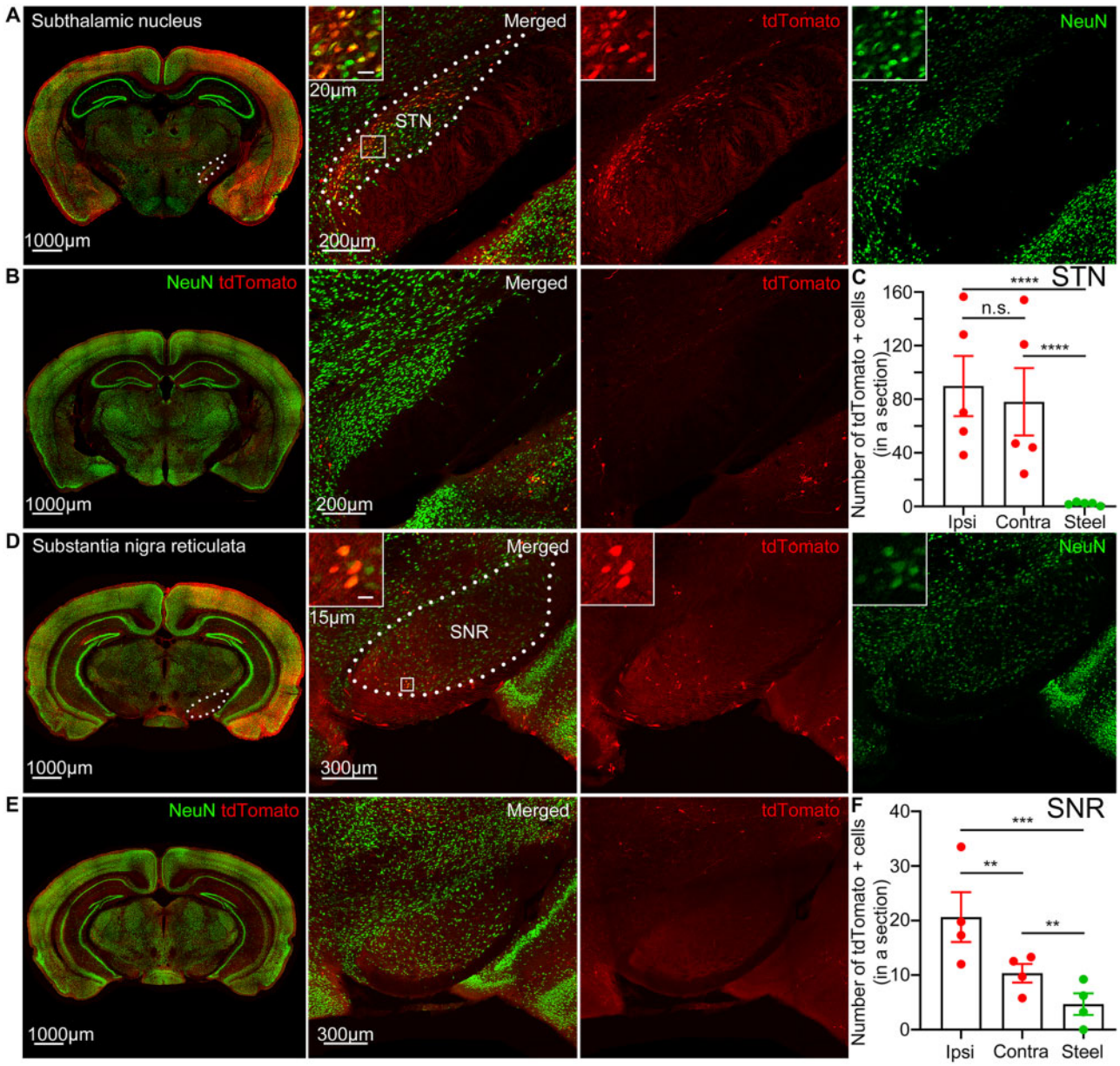

Figure 5 Seizures activate the subthalamic nucleus and substantia nigra pars reticulate. (**A**) tdTomato expression in the STN immunolabelled for NeuN (green) and its magnified view. *Boxed inset*: tdTomato-positive neurons co-localized with NeuN. Dotted lines indicate the STN boundaries. (**B**) *Left*: Steel wire control showed minimal tdTomato expression in the STN. *Right*: Magnified view of the STN. (**C**) Cobalt-implanted mice had more tdTomato-positive cells in the ipsilateral and contralateral STN compared to the steel wire control mice (each point is the average number of cells in a 40 μm section across sequential STN sections in a mouse) (ipsilateral: 89.90 ± 22.49 cells, unpaired *t*-test; contralateral: 78.11 ± 25.15 cells, unpaired *t*-test; control: 2.030 ± 0.5463 cells; $n = 5$ mice). The number of tdTomato-positive cells in the ipsilateral STN was similar to that in the contralateral (unpaired *t*-test). (**D**) tdTomato expression in the SNR immunolabelled for NeuN (green) and its magnified view. *Boxed inset*: tdTomato-positive neurons co-localized with NeuN. Dotted lines indicate the SNR boundaries. (**E**) *Left*: Steel wire control showed minimal tdTomato expression in the SNR. *Right*: Magnified view of the SNR. (**F**) Cobalt-implanted mice had more tdTomato-positive cells in both ipsilateral and contralateral SNR compared to the steel wire implanted mice (each point is the average number of cells in a 40 μm section across sequential SNR sections in a mouse) (ipsilateral: 20.65 ± 4.580 cells, $P = 0.0005$, unpaired *t*-test; contralateral: 10.36 ± 1.704 cells, $P = 0.0029$, unpaired *t*-test; control: 4.688 ± 1.985 cells; $n = 4$ mice). The ipsilateral SNR had more tdTomato-positive cells than the contralateral in mice with seizures ($P = 0.0010$, unpaired *t*-test). Data are mean ± SEM, n.s. = non-significant. ** $P < 0.01$, *** $P < 0.001$, **** $P < 0.0001$.

indicate that the ipsilateral striatum was also active and synchronized with the cortex because the motor cortex projects directly to the striatum (Supplementary Fig. 2).

Light-sheet microscopy allowed us to visualize viral spread in a whole unsliced brain of a TRAP mouse after secondarily generalized seizures. Three-dimensional rendering of the brain revealed the structure of AAV9-GFP-positive axons that ran posteriorly through the striatum (Fig. 8C and Supplementary Video 3).

GFP and tdTomato also co-localized throughout the ipsilateral GPe (Fig. 8E). tdTomato-positive fibres expressed GFP as they ran dorsally in the GPe, a part of the indirect pathway. AAV9 Cre-independent virus does not cross more than one synapse,[62] which means parallel projections exist directly from the motor cortex to the GPe in addition to the striatal projections to the GPe. Previous literature supports that direct cortico-pallidal projections exist.[63–65]

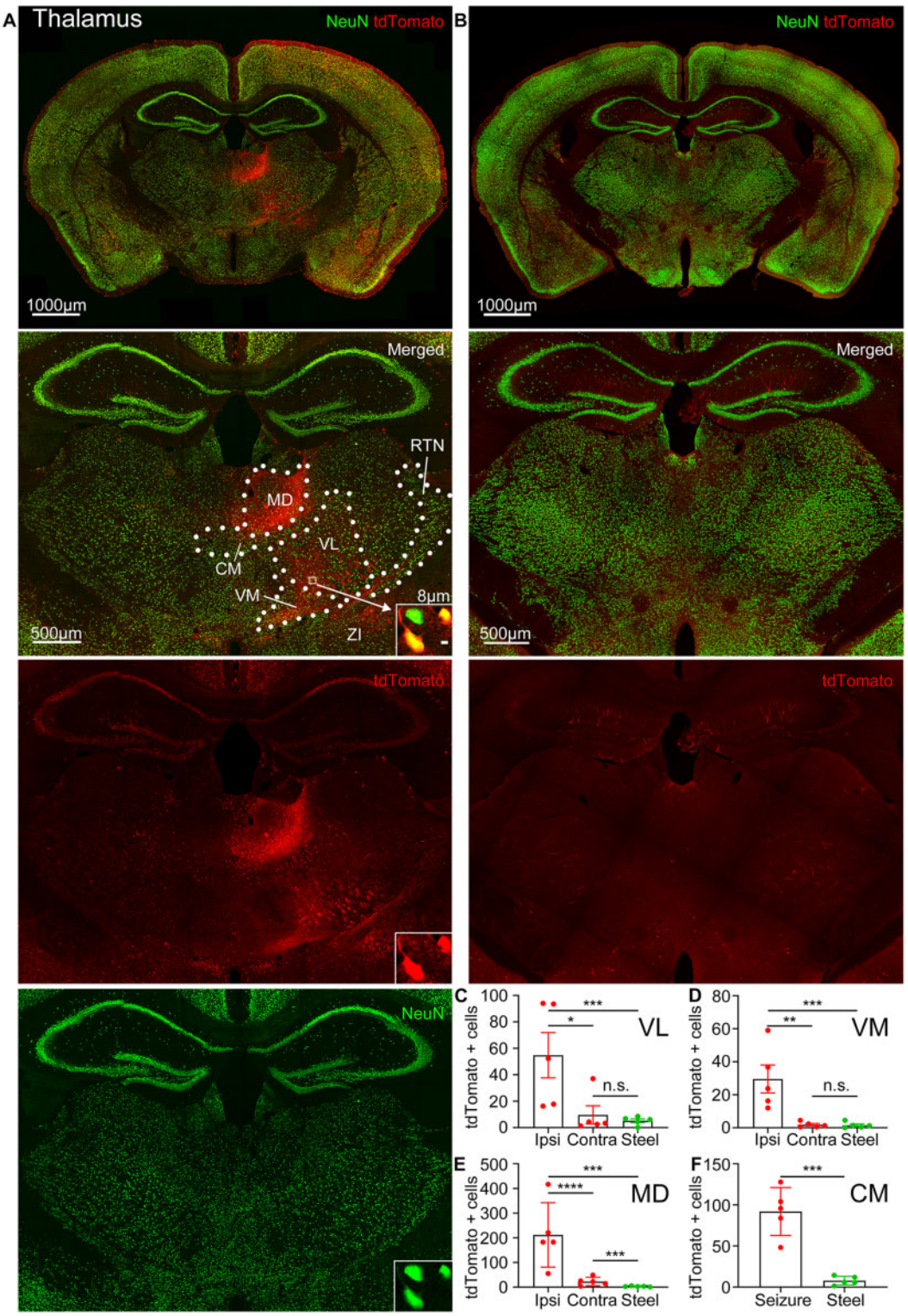

Figure 6 Seizures activate motor thalamic nuclei. (**A**) *Top*: tdTomato expression in the thalamus immunolabelled for NeuN (green). *Bottom*: Magnified view of the thalamus. *Boxed inset* (white arrow): tdTomato-positive neurons co-localized with NeuN. Dotted lines indicate nuclear boundaries: CM = centromedian; MD = mediodorsal; RTN = reticular thalamic nucleus; ZI = zona incerta. (**B**) *Top*: Steel wire control showed minimal tdTomato expression in the thalamus. *Bottom*: Magnified view of the thalamus. (**C–F**) Number of tdTomato-positive cells in cobalt-implanted mice (red) compared to the steel wire implanted mice (green) in the thalamic nuclei VL, VM, mediodorsal thalamic nucleus, and centromedian thalamic nucleus [either on the ipsilateral (Ipsi) or contralateral (Contra) side to the seizure focus or, in the case of the centromedian thalamic nucleus, in the whole nucleus (Seizure)], (each point is the average number of cells in a 40 µm section across sequential nuclear sections in a mouse) [VL: ipsilateral: 54.77 ± 17.17 cells, $P = 0.0006$, unpaired *t*-test; contralateral: 9.667 ± 6.850 cells, unpaired *t*-test; control: 5.183 ± 1.417 cells; $n = 5$ mice; the ipsilateral VL had more tdTomato-positive cells than the contralateral ($P = 0.0194$, unpaired *t*-test); VM: ipsilateral: 29.55 ± 8.469 cells, $P = 0.0008$, Kolmogorov-Smirnov test; contralateral: 1.833 ± 0.7472 cells, Kolmogorov-Smirnov test; control: 1.508 ± 0.7932 cells; $n = 5$ mice; the ipsilateral VM had more tdTomato-positive cells than the contralateral ($P = 0.0033$, unpaired *t*-test); mediodorsal thalamic nucleus: ipsilateral: 211.6 ± 58.51 cells, $P = 0.0006$, Kolmogorov-Smirnov test; contralateral: 22.65 ± 7.437 cells, $P = 0.0006$, Kolmogorov-Smirnov test; control: 2.749 ± 0.8787 cells; $n = 5$ mice; the ipsilateral mediodorsal thalamic nucleus had more tdTomato-positive cells than the contralateral (unpaired *t*-test); centromedian thalamic nucleus: whole nucleus (Seizure): 91.97 ± 13.07 cells, $P = 0.0002$, unpaired *t*-test; control: 7.778 ± 2.338 cells; $n = 5$ mice]. Data are mean ± SEM, Kolmogorov-Smirnov test, n.s. = non-significant. $^{*}P < 0.05$, $^{**}P < 0.01$, $^{***}P < 0.001$, $^{****}P < 0.0001$.

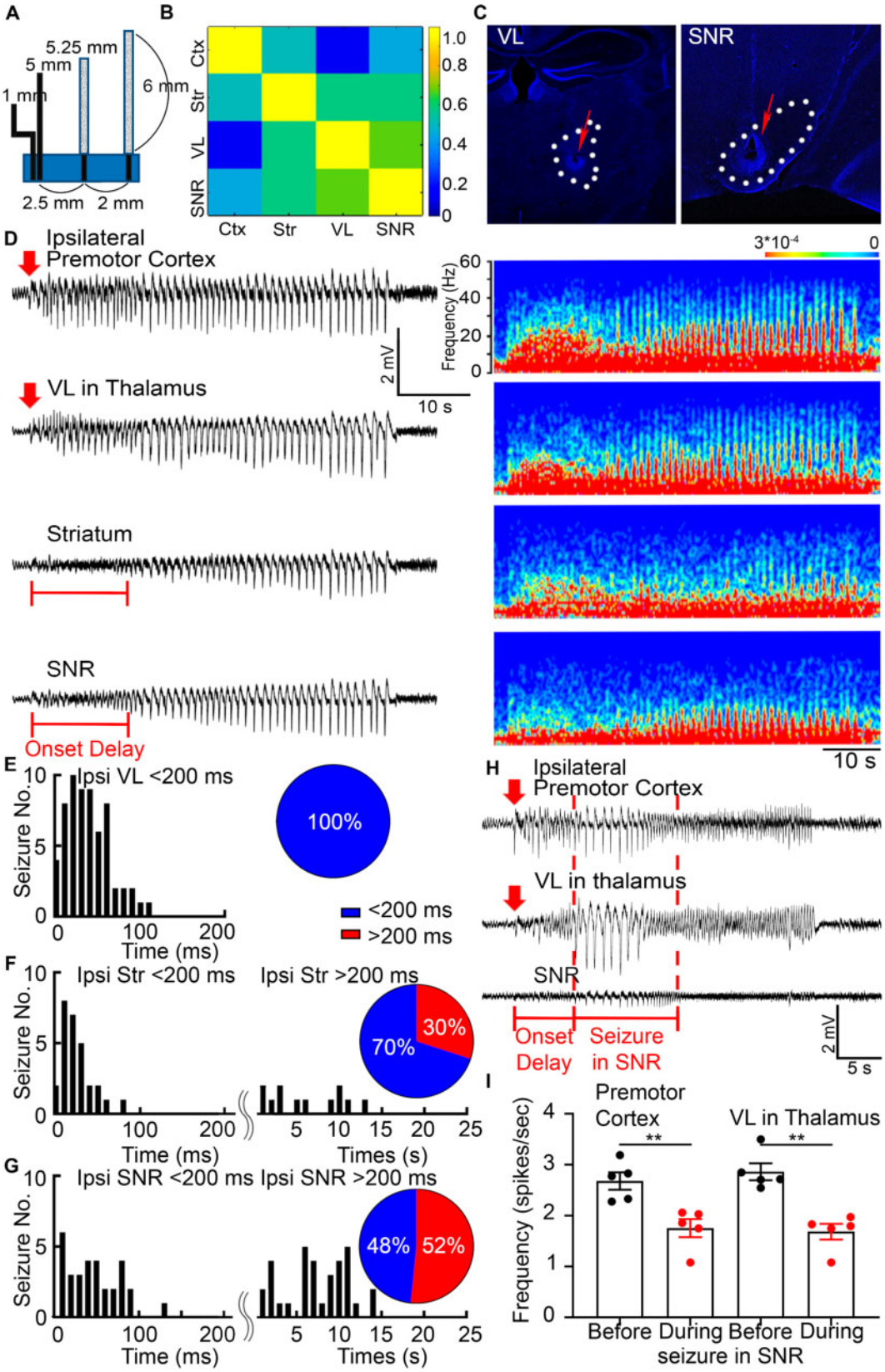

Figure 7 Activation of the basal ganglia modulates seizures. (**A**) Custom-made arrays of LFP microelectrodes that record from the ipsilateral premotor cortex, striatum, VL, and SNR and their dimensions for stereotaxic surgery. (**B**) A correlation matrix plots the correlation coefficients (from 1.0 to 0) for each pair of structures, which were calculated based on the LFP time lags between the microelectrodes with the dimensions from (**A**) and 60–75 kΩ resistance. (**C**) Lesions were done after the recordings to mark the locations of the microelectrode tips that targeted the VL and SNR (red arrows). (**D**) Representative simultaneous LFP recordings from the premotor cortex, VL, striatum, and SNR and their corresponding power spectrums. The seizure focus was in the premotor cortex. Red arrows indicate seizure onset time (twice the baseline). Red bars in the striatum and SNR indicate

(continued)

Next, we injected Cre-driven AAV9 pCAG-FLEX-EGFP-WPRE in TRAP2 mice at the seizure focus, so that the virus would only be expressed in activated neurons and axons. We found GFP and tdTomato co-localization in the striatum and GPe (Fig. 8F). We did not find viral expression in the GPi, and cerebral peduncle and zona incerta expressed the virus close to the STN and SNR (Fig. 8F).

Discussion

Our studies, for the first time, map neuronal activation of the basal ganglia during frontal lobe focal motor to bilateral seizures with unprecedented spatial resolution. This map suggests at least two possibilities that seizures either activate structures of the basal ganglia and indirect pathway neurons directly from the cortex or propagate along the indirect pathway sequentially. Our studies could not distinguish between these two possibilities, so future experiments with calcium imaging, chemogenetics, and other techniques will be necessary to distinguish these possibilities. We show that seizures originating in the premotor cortex activate anatomically connected structures on the mesoscale and cellular levels: striatum, globus pallidus, subthalamic nucleus, substantia nigra, and the thalamus, which suggests that neuronal connections play a role in seizure spread.

We show striatal activation during frontal lobe secondarily generalized tonic-clonic seizures. Furthermore, around 80% of all activated neurons in the striatum during focal to bilateral seizures expressed D2 receptors, and the D2 agonist exerted an anticonvulsant effect. These findings indicate that the indirect system modulates seizures similar to how the physiological activation of the indirect pathway suppresses motor movement.[49] The TRAP technique lacks temporal resolution and represents the activity of neurons over ∼90 min, but seizures occur over 10–180 s, a much shorter timescale. Physiological brain activity causes TRAPing of neurons, and the rate of activation of c-Fos can vary from region to region. To complement TRAP spatial resolution and gain temporal resolution, we recorded LFPs and found that seizures activate structures via short and long latency loops, and activation of the basal ganglia modulates seizures. Seizures originating in the frontal lobe, the second most common site of seizure foci after the temporal lobe, follow the anatomical connections of the motor cortex, so anatomical projections of the epileptic focus influence the seizure circuit.

Hughlings Jackson originally proposed that the motor cortex generates seizures,[1] and seminal studies of Jasper and Penfield demonstrated seizure-induced reorganization of the motor cortex.[66] The striatum is the key output structure of the motor cortex. Studies in the 1980s suggested that basal ganglia participate in seizures,[4,67,68] and dopaminergic drugs modulate them.[12] Previous studies also reported electrographic activation of the striatum during focal and absence seizures[7,9,69] and hyperactivity of striatal neurons after amygdala-kindled temporal lobe seizures.[70] However, these studies did not provide spatial and temporal resolution of the current study.[6,8]

We used the cobalt model to induce frontal lobe secondarily generalized seizures.[15–17,19] We selected this model over others for several reasons. The cobalt model provides reliable, spontaneous seizures in >90% of animals. The short latency allows us to obtain high fidelity LFP recordings because electrical contacts do not deteriorate. These seizures are consistently associated with focal onset electrographic spike-wave discharges and beta-gamma bursts of activity. Anticonvulsant drugs such as carbamazepine and phenytoin suppress these seizures as they do in human focal motor seizures.[71] Although electrical stimulation of the cortex or application of chemiconvulsants (e.g. 4-aminopyridine or penicillin) are also models of focal seizures, these are the models of acute rather than spontaneous seizures and require prolonged electrical stimulation or introduce a bias towards a cortical layer in which seizures originate. Cortical freeze lesion or undercut models do not provide a reliable seizure phenotype, and the latency period spans weeks before the first seizures appear.[72] However, the cobalt model has limitations as well: it creates a lesion near cobalt implantation, seizures stop in 2–3 days, and it is not a model of epileptogenesis. The current study did not investigate epileptogenesis but studied seizure circuits.

We provide direct evidence that motor seizures activate the structures that are anatomically connected to the seizure focus and between each other, suggesting that subcortical seizure spread is influenced by connectivity. Our findings are similar to a previous study that mapped the effects of artificial electrical stimulation of the motor cortex without inducing seizures. Parthasarathy and Graybiel[73] found c-Fos expression in the striatum, GPe, STN, and the reticular thalamic nucleus, but not in the GPi. They found that out of all c-Fos-positive cells in the striatum, 75% of them expressed enkephalin, suggesting preferential activation of the indirect pathway over the direct during sensorimotor cortical stimulation without seizures.[73]

A recent study of seizure spread from the visual cortex, combining *in vivo* imaging and electrophysiology, demonstrated that seizures follow anatomical connections of the visual cortex.[74,75] Our studies show that seizures originating in the premotor cortex activate anatomically connected subcortical basal ganglia structures, preferentially activating DRD2 neurons. D2-expressing medium spiny neurons (MSNs) of the indirect pathway are more excitable than D1 MSNs.[76] D2 MSNs have a smaller surface area and dendritic trees and a less hyperpolarized resting membrane potential compared to those of D1 MSNs, which explains higher responsiveness of D2 MSNs to current injections[76,77] and, as we found, easier and greater activation of D2 MSNs during seizures. Higher excitability of D2 neurons also suggests that properties of neurons in addition to connectivity determine the pattern of neuronal activation during seizures.

Figure 7 Continued
the delay of seizure onset. (**E**) Seizure onset times (ms) in the ipsilateral VL after the beginning of seizures in the premotor cortex. Pie chart: 100% of seizures required <200 ms to arrive at the VL from the premotor cortex (blue): 33.0095 ± 3.1550 ms, n = 63 seizures from 16 mice. (**F**) Seizure onset times (ms or s) in the ipsilateral striatum after the beginning of seizures in the premotor cortex. Pie chart: 70% of seizures required <200 ms to arrive to the striatum from the premotor cortex (blue): 19.6643 ± 3.5197 ms, n = 28 seizures from eight mice, and 30% of seizures required >200 ms (red): 5.7125 ± 1.1929 s, n = 12 seizures from four mice. (**G**) Seizure onset times (ms or s) in the ipsilateral SNR after the beginning of seizures in the premotor cortex. Pie chart: 48% of seizures required <200 ms to arrive to the SNR from the premotor cortex: 41.8526 ± 5.4110 ms, n = 31 seizures from 12 mice, and 52% of seizures required >200 ms (red): 6.9970 ± 0.6562 s, n = 33 seizures from 11 mice. (**H**) Simultaneous LFP recordings from the ipsilateral premotor cortex, VL, and SNR. Spike frequency drops in the premotor cortex and VL after seizure appears in the SNR (red bar and dashed vertical lines). Red arrows indicate seizure onset time. (**I**) Spike frequency quantification (spikes/s) in the premotor cortex and VL before seizure in the SNR (black) and during seizure in the SNR (red) (premotor cortex before seizure in SNR: 2.682 ± 0.1699 spikes/s; premotor cortex during seizure in SNR: 1.756 ± 0.1782 spikes/s; P = 0.0055, unpaired t-test; VL before: 2.866 ± 0.1656 spikes/s; VL during: 1.687 ± 0.1563 spikes/s; P = 0.0079, Kolmogorov-Smirnov test; n = 12 seizures from four mice). Data are mean ± SEM, $^{**}P < 0.01$.

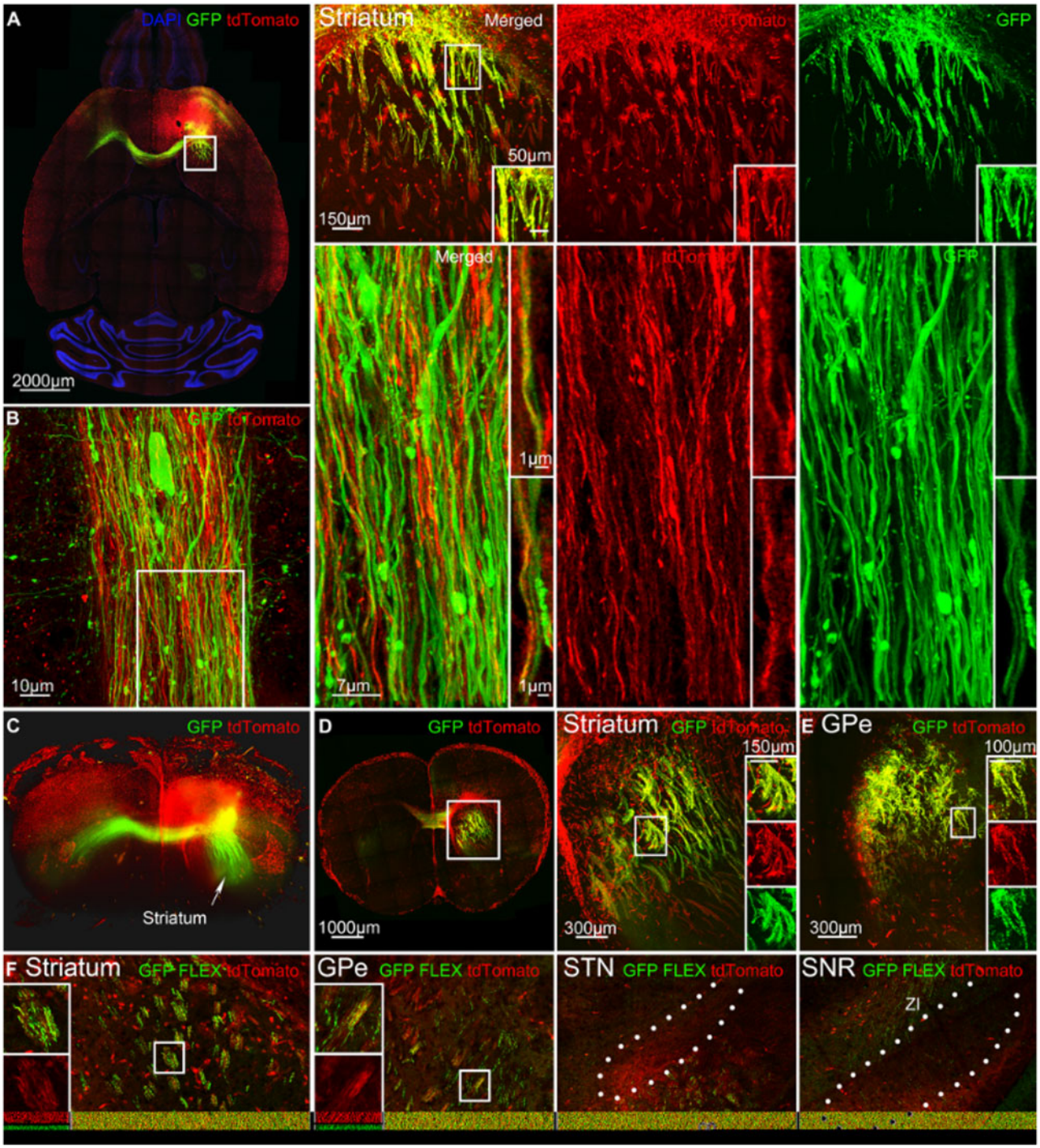

Figure 8 Anatomical connections of the seizure focus influence seizure circuit. (**A**) *Left*: A horizontal section shows AAV9-CamKII0.4.eGFP.WPRE.Rbg virus (green) labelling anatomical projections of the seizure focus in the premotor cortex and tdTomato expression (red) after focal motor to bilateral tonic-clonic seizure. *Right*: Magnified view of the viral expression in the striatum ipsilateral to the seizure focus. *Boxed inset*: Cobalt-localization of tdTomato-positive axons and AAV9-GFP. (**B**) *Left*: SP8 super-resolution lightning microscopy image of a horizontal axonal bundle in the striatum that expresses AAV9-GFP and tdTomato. *Right*: Magnified view of the axonal bundle. *Boxed insets*: Cobalt-localization of tdTomato-positive axons and AAV9-GFP. (**C**) Light-sheet microscopy 3D image of one-third of the clarified brain that expresses AAV9-GFP from the seizure focus and tdTomato. The white arrow indicates striatal axons that run posteriorly from the seizure focus. (**D**) *Left*: Clarified 200 µm section of the striatum that expresses AAV9-GFP and tdTomato in the striatum. *Right*: Magnified view of the striatum. *Boxed insets*: tdTomato-positive axons co-localized with AAV9-GFP. (**E**) Clarified 200 µm section of the GPe that expresses AAV9-GFP and tdTomato. *Boxed insets*: tdTomato-positive fibres co-localized with AAV9-GFP. (**F**) Cre-driven AAV9 (pCAG-FLEX-EGFP-WPRE) was injected in TRAP2 mice at the seizure focus in the premotor cortex. The striatum and GPe expressed Cre-driven virus as well as the cerebral peduncle (cp) and zona incerta (ZI) near STN and SNR. Also, see Supplementary Videos 2 and 3.

We found strong tdTomato expression in the GPe, yet the striatum sends GABAergic projections and inhibits it. Similarly, motor thalamic nuclei VM/VL expressed tdTomato, but the SNR inhibits VM/VL.[57] The activation of the GPe and VM/VL could be explained by the existence of direct, parallel cortico-pallidal and cortico-thalamic projections as indicated by the viral expression in the GPe

(Fig. 8E) and previous studies.[58,65] Although activation of the indirect pathway neurons inhibits prototypic GPe neurons, disinhibiting STN and arkypallidal GPe neurons[56] (Fig. 4B), our study could not distinguish whether the observed activation of these basal ganglia structures is a result of the direct cortical excitation or a sequential flow of excitation through the indirect pathway. Future experiments will be necessary to address this.

The canonical circuit posits that focal seizures engage the thalamocortical circuit, which leads to secondarily generalized tonic-clonic seizures.[78–85] Even though we studied secondarily generalized seizures, we did not investigate the mechanism behind secondary generalization (or bilateral spread). We observed profound activation of the motor and mediodorsal thalamic nucleus thalamic nuclei, which might play a key role in generalized seizures. Here, we report basal ganglia activation on the cellular level in addition to the thalamus, which suggests that the seizure circuit might be more complex and driven by the properties of neurons and connectivity with multiple, parallel pathways active.

It is essential to understand the neural circuits supporting these seizures because frontal lobe epilepsy is the second most common type of epilepsy. Repeated generalized tonic-clonic seizures are the leading risk factor for sudden unexpected death in epilepsy (SUDEP)[86] and lead to fractures and soft tissue injuries.[87] Understanding the neuronal circuits that generate and propagate these seizures will allow for the development of novel therapeutic approaches. Injection of an excitatory amino acid derivative N-Methyl-D-aspartate (NMDA) into the striatum protects against limbic pilocarpine seizures, whereas striatal lesioning worsens seizures.[88] Low-frequency striatal stimulation had an anti-epileptic effect in 57 patients with pharmaco-resistant temporal lobe epilepsy.[89,90] Previous studies also suggest that the SNR is critically involved in seizure generalization.[5] ^{14}C-2-deoxyglucose metabolic mapping studies found involvement of the SNR in motor seizures.[4,68] Infusion of muscimol, GABA receptor agonist, into the SNR produces anticonvulsant effect,[67,91] and SNR lesions are anticonvulsant too.[92] High-frequency stimulation of the STN also led to a reduction in seizure frequency in patients with drug-resistant epilepsy.[93] STN high-frequency stimulation decreases the activity of the SNR and induces its functional inhibition.[94,95] Low concentrations of dopamine in the striatum have been shown to produce depolarization and increased frequency of spontaneous firing, whereas high concentrations inhibited spontaneous firing.[12] Despite this complex dual effect, D2 agonist or the release of dopamine is thought to reduce activity along the indirect pathway and reduce SNR activity,[60] potentially explaining the anticonvulsant effect of D2 agonists. During seizures, however, we found activation of the STN and SNR.

Our study generates new targets for modulation of seizures by deep brain stimulation. Currently, patients with refractory epilepsy are treated with the anterior thalamic nucleus and responsive neurostimulation.[96] In the future, multiple subcortical structures could be targeted for modulation, stimulation, resection, or medications. Overall, our studies provide the precise neuronal activity map of frontal lobe focal to bilateral tonic-clonic seizures, revealing a richly complex circuit subject to modulation by the basal ganglia.

Acknowledgements

Super-resolution Leica SP8 STED, Zeiss LSM 980 multiphoton Airyscan 2, and Zeiss Light Sheet imaging were performed at the University of Virginia W.M. Keck Center for Cellular Imaging, which is supported by NIH-OD025156. We also thank John Williamson, Ruth Stornetta, Alev Erisir, Howard Goodkin, Mark Beenhakker, and Daniel Weller, and the rest of the Kapur lab for valuable comments on this study.

Funding

This work was supported by the National Institute of Health (RO1 NS040337, RO1 NS044370 to J.K.) and the UVA Brain Institute.

Competing interests

The authors report no competing interests.

Supplementary material

Supplementary material is available at *Brain* online.

References

1. Hughlings Jackson J. The Lumleian Lectures on convulsive seizures. *Lancet*. 1890;135(3476):785–788.
2. Shepherd GMG. Corticostriatal connectivity and its role in disease. *Nat Rev Neurosci*. 2013;14(4):278–291.
3. Engel J, Wolfson L, Brown L. Anatomical correlates of electrical and behavioral events related to amygdaloid kindling. *Ann Neurol*. 1978;3(6):538–544.
4. Lothman EW, Collins RC. Kainic acid induced limbic seizures: Metabolic, behavioral, electroencephalographic and neuropathological correlates. *Brain Res*. 1981;218(1-2):299–318.
5. Velíšková J, Moshé SL. Update on the role of substantia nigra pars reticulata in the regulation of seizures. *Epilepsy Curr*. 2006; 6(3):83–87.
6. Blumenfeld H, Varghese GI, Purcaro MJ, et al. Cortical and subcortical networks in human secondarily generalized tonic-clonic seizures. *Brain*. 2009;132(Pt 4):999–1012.
7. Devergnas A, Piallat B, Prabhu S, et al. The subcortical hidden side of focal motor seizures: Evidence from micro-recordings and local field potentials. *Brain*. 2012;135(Pt 7):2263–2276.
8. He X, Chaitanya G, Asma B, et al. Disrupted basal ganglia-thalamocortical loops in focal to bilateral tonic-clonic seizures. *Brain*. 2020;143(1):175–190.
9. Miyamoto H, Tatsukawa T, Shimohata A, et al. Impaired cortico-striatal excitatory transmission triggers epilepsy. *Nat Commun*. 2019;10(1):1917.
10. Calabresi P, Picconi B, Tozzi A, Ghiglieri V, Filippo mediodorsal thalamic nucleus. Direct and indirect pathways of basal ganglia: A critical reappraisal. *Nat Neurosci*. 2014;17(8):1022–1030.
11. Gerfen CR, Surmeier DJ. Modulation of striatal projection systems by dopamine. *Annu Rev Neurosci*. 2011;34:441–466.
12. Turski L, Cavalheiro EA, Bortolotto ZA, Ikonomidou-Turski C, Kleinrok Z, Turski WA. Dopamine-sensitive anticonvulsant site in the rat striatum. *J Neurosci*. 1988;8(11):4027–4037.
13. Allen WE, DeNardo LA, Chen MZ, et al. Thirst-associated preoptic neurons encode an aversive motivational drive. *Science*. 2017;357(6356):1149–1155.
14. Guenthner CJ, Miyamichi K, Yang HH, Craig Heller H, Luo L. Permanent genetic access to transiently active neurons via TRAP: Targeted recombination in active populations. *Neuron*. 2013;78(5):773–784.
15. Grimm RJ, Frazee JG, Kawasaki T, Savić M. Cobalt epilepsy in the squirrel monkey. *Electroencephalogr Clin Neurophysiol*. 1970;29(5): 525–528.
16. Hartman ER, Colasanti BK, Craig CR. Epileptogenic properties of cobalt and related metals applied directly to cerebral cortex of rat. *Epilepsia*. 1974;15(1):121–129.

17. Henjyoji EY, Dow RS. Cobalt-induced seizures in the cat. *Electroencephalogr Clin Neurophysiol*. 1965;19(2):152–161.
18. Singh T, Joshi S, Williamson JM, Kapur J. Neocortical injury–induced status epilepticus. *Epilepsia*. 2020;61(12):2811–2824.
19. Kim J, Woo J, Park Y-G, et al. Thalamic T-type Ca2 + channels mediate frontal lobe dysfunctions caused by a hypoxia-like damage in the prefrontal cortex. *J Neurosci*. 2011;31(11):4063–4073.
20. André V, Pineau N, Motte JE, Marescaux C, Nehlig A. Mapping of neuronal networks underlying generalized seizures induced by increasing doses of pentylenetetrazol in the immature and adult rat: A c-Fos immunohistochemical study. *Eur J Neurosci*. 1998;10(6):2094–2106.
21. Labiner DM, Butler LS, Cao Z, Hosford DA, Shin C, Mcnamara Jo. Induction of c-fos mRNA by kindled seizures: Complex relationship with neuronal burst firing. *J Neurosci*. 1993;13(2):744–751.
22. Morgan JI, Cohen DR, Hempstead JL, Curran T. Mapping patterns of c-fos expression in the central nervous system after seizure. *Science*. 1987;237(4811):192–197.
23. Peng Z, Houser CR. Temporal patterns of Fos expression in the dentate gyrus after spontaneous seizures in a mouse model of temporal lobe epilepsy. *Neurobiol Dis*. 2005;25(31):7210–7220.
24. Graybiel AM, Ragsdale CW. Histochemically distinct compartments in the striatum of human, monkey, and cat demonstrated by acetylthiocholinesterase staining. *Proc Nati Acad Sci U S A*. 1978;75(11):5723–5726.
25. Smith JB, Klug JR, Ross DL, et al. Genetic-based dissection unveils the inputs and outputs of striatal patch and matrix compartments. *Neuron*. 2016;91(5):1069–1084.
26. Clasadonte J, Haydon PG. Astrocytes and epilepsy. In: Noebels JL, Avoli M, Rogawski MA, eds. *Jasper's basic mechanisms of the epilepsies*. US: National Center for Biotechnology Information; 2012:591–605.
27. Wahnschaffe U, Löscher W. Anticonvulsant effects of ipsilateral but not contralateral microinjections of the dopamine D2 agonist LY 171555 into the nucleus accumbens of amygdala-kindled rats. *Brain Res*. 1991;553(2):181–187.
28. Turski WA, Cavalheiro EA, Ikonomidou C, Bortolotto ZA, Klockgether T, Turski L. Dopamine control of seizure propagation: Intranigral dopamine D1 agonist SKF-38393 enhances susceptibility to seizures. *Synapse*. 1990;5(2):113–119.
29. Alper K, Schwartz KA, Kolts RL, Khan A. Seizure incidence in psychopharmacological clinical trials: An analysis of Food and Drug Administration (FDA) summary basis of approval reports. *Biol Psychiatry*. 2007;62(4):345–354.
30. Behere RV, Anjith D, Rao NP, Venkatasubramanian G, Gangadhar BN. Olanzapine-induced clinical seizure: A case report. *Clin Neuropharmacol*. 2009;32(5):297–298.
31. Koch-Stoecker S. Antipsychotic drugs and epilepsy: Indications and treatment guidelines. *Epilepsia*. 2002;43(s2):19–24.
32. Uvais NA, Sreeraj VS. Seizure associated with olanzapine. *J Fam Med Prim Care*. 2018;7:1090–1092.
33. Barone P, Lamb J, Ellis A, Clarke Z.Sumanirole versus placebo or ropinirole for the adjunctive treatment of patients with advanced Parkinson's disease. *Mov Disord*. 2007;22(4):483–489.
34. Durham RA, Eaton MJ, Moore KE, Lookingland KJ. Effects of selective activation of dopamine D2 and D3 receptors on prolactin secretion and the activity of tuberoinfundibular dopamine neurons. *Eur J Pharmacol*. 1997;335(1):37–42.
35. McCall RB, Lookingland KJ, Bédard PJ, Huff RM. Sumanirole, a highly dopamine D2-selective receptor agonist: In vitro and in vivo pharmacological characterization and efficacy in animal models of Parkinson's disease. *J Pharmacol Exp Ther*. 2005;314(3):1248–1256.
36. Sethy VH, Ellerbrock BR, Wu H. U-95666E: A potential anti-Parkinsonian drug with anxiolytic activity. *Prog Neuro Psychopharmacol Biol Psychiatry*. 1997;21(5):873–883.
37. Singer C, Lamb J, Ellis A, Layton G.;; Sumanirole for Early Parkinson's Disease Study Group. A comparison of sumanirole versus placebo or ropinirole for the treatment of patients with early Parkinson's disease. *Mov Disord*. 2007;22(4):476–482.
38. Stojanovic T, Orlova M, Sialana FJ, et al. Validation of dopamine receptor DRD1 and DRD2 antibodies using receptor deficient mice. *Amino Acids*. 2017;49(6):1101–1109.
39. Curran EJ, Watson SJ. Dopamine receptor mRNA expression patterns by opioid peptide cells in the nucleus accumbens of the rat: A double in situ hybridization study. *J Comp Neurol*. 1995;361(1):57–76.
40. Gerfen CR, Engber TM, Mahan LC, et al. D1 and D2 dopamine receptor-regulated gene expression of striatonigral and striatopallidal neurons. *Science*. 1990;250(4986):1429–1432.
41. Deng YP, Lei WL, Reiner A. Differential perikaryal localization in rats of D1 and D2 dopamine receptros on striatal projection neuron types identified by retrograde labeling. *J Chem Neuroanat*. 2006;32(2-4):101–116.
42. Harrison MB, Wiley RG, Wooten GF. Selective localization of striatal D1 receptors to striatonigral neurons. *Brain Res*. 1990;528(2):317–322.
43. Harrison MB, Wiley RG, Wooten GF. Changes in D2 but not D1 receptor binding in the striatum following a selective lesion of striatopallidal neurons. *Brain Res*. 1992;590(1-2):305–310.
44. Le Moine C, Normand E, Guitteny AF, Fouque B, Teoule R, Bloch B. Dopamine receptor gene expression by enkephalin neurons in rat forebrain. *Proc Natl Acad Sci U S A*. 1990;87(1):230–234.
45. Pollack AE, Harrison MB, Wooten GF, Fink JS. Differential localization of A2a adenosine receptor mRNA with D1 and D2 dopamine receptor mRNA in striatal output pathways following a selective lesion of striatonigral neurons. *Brain Res*. 1993;631(1):161–166.
46. Hersch SM, Ciliax BJ, Gutekunst C-A, et al. Electron microscopic analysis of Dl and D2 dopamine receptor proteins in the dorsal striatum and their synaptic relationships with motor corticostriatal afferents. *J Neurosci*. 1995;15(7):5222–5237.
47. Le Moine C, Bloch B. D1 and D2 dopamine receptor gene expression in the rat striatum: Sensitive cRNA probes demonstrate prominent segregation of D1 and D2 mRNAs in distinct neuronal populations of the dorsal and ventral striatum. *J Comp Neurol*. 1995;355(3):418–426.
48. Gong S, Zheng C, Doughty ML, et al. A gene expression atlas of the central nervous system based on bacterial artificial chromosomes. *Nature*. 2003;425(6961):917–925.
49. Kravitz AV, Freeze BS, Parker PRL, et al. Regulation of parkinsonian motor behaviours by optogenetic control of basal ganglia circuitry. *Nature*. 2010;466(7306):622–626.
50. Lee HJ, Weitz AJ, Bernal-Casas D, et al. Activation of direct and indirect pathway medium spiny neurons drives distinct brain-wide responses. *Neuron*. 2016;91(2):412–424.
51. Franklin KBJ, Paxinos G. Paxinos and Franklin's the mouse brain in stereotaxic coordinates, 4th edn. Academic Press; 2012.
52. Abdi A, Mallet N, Mohamed FY, et al. Prototypic and arkypallidal neurons in the dopamine-intact external globus pallidus. *J Neurosci*. 2015;35(17):6667–6688.
53. Boley AM, Perez SM, Lodge DJ. A fundamental role for hippocampal parvalbumin in the dopamine hyperfunction associated with schizophrenia. *Schizophr Res*. 2014;157(1-3):238–243.
54. Dodson PD, Larvin JT, Duffell JM, et al. Distinct developmental origins manifest in the specialized encoding of movement by adult neurons of the external Globus pallidus. *Neuron*. 2015;86(2):501–513.
55. Saunders A, Huang KW, Sabatini BL. Globus pallidus externus neurons expressing parvalbumin interconnect the subthalamic

nucleus and striatal interneurons. *PLoS One*. 2016;11(2): e0149798.
56. Ketzef M, Silberberg G. Differential synaptic input to external globus pallidus neuronal subpopulations in vivo. *Neuron*. 2020; 109(3):516–529.e4.
57. Solomon IC, Halat TJ, El-Maghrabi R, O'Neal MH. Projections from the substantia nigra pars reticulata to the motor thalamus of the rat: Single axon reconstructions and immunohistochemical study. *J Comp Neurol*. 2001;440:20–30.
58. Hooks BM, Mao T, Gutnisky DA, Yamawaki N, Svoboda K, Shepherd GMG. Organization of cortical and thalamic input to pyramidal neurons in mouse motor cortex. *J Neurosci*. 2013; 33(2):748–760.
59. Terlau J, Yang J, Khastkhodaei Z, et al. Spike-wave discharges in absence epilepsy: Segregation of electrographic components reveals distinct pathways of seizure activity. *J Physiol*. 2020; 598(12):2397–2414.
60. DeLong MR, Wichmann T. Circuits and circuit disorders of the basal ganglia. *Arch Neurol*. 2007;64(1):20–24.
61. Yang B, Treweek JB, Kulkarni RP, et al. Single-cell phenotyping within transparent intact tissue through whole-body clearing. *Cell*. 2014;158(4):945–958.
62. Zingg B, Chou X-L, Zhang Z-G, et al. AAV-mediated anterograde transsynaptic tagging: Mapping corticocollicular input-defined neural pathways for defense behaviors. *Neuron*. 2017;93(1): 33–47.
63. Chen MC, Ferrari L, Sacchet mediodorsal thalamic nucleus, et al. Identification of a direct GABAergic pallidocortical pathway in rodents. *Eur J Neurosci*. 2015;41(6):748–759.
64. Grewal SS, Holanda VM, Middlebrooks EH. Corticopallidal connectome of the globus pallidus externus in humans: An exploratory study of structural connectivity using probabilistic diffusion tractography. *Am J Neuroradiol*. 2018; 39(11):2120–2125.
65. Karube F, Takahashi S, Kobayashi K, Fujiyama F. Motor cortex can directly drive the globus pallidus neurons in a projection neuron type-dependent manner in the rat. *Elife*. 2019;8:1–25.
66. Penfield W, Jasper HH. Epilepsy and the functional anatomy of the human brain. Boston: Little, Brown; 1954.
67. Iadarola MJ, Gale K. Substantia nigra: Site of anticonvulsant activity mediated by γ-aminobutyric acid. *Science*. 1982;218(4578): 1237–1240.
68. Velíšková J, Miller AM, Nunes ML, Brown LL. Regional neural activity within the substantia nigra during peri-ictal flurothyl generalized seizure stages. *Neurobiol Dis*. 2005;20(3):752–759.
69. Aupy J, Wendling F, Taylor K, Bulacio J, Gonzalez-Martinez J, Chauvel P. Cortico-striatal synchronization in human focal seizures. *Brain*. 2019;142(5):1282–1295.
70. Kücker S, Töllner K, Piechotta M, Gernert M. Kindling as a model of temporal lobe epilepsy induces bilateral changes in spontaneous striatal activity. *Neurobiol Dis*. 2010;37(3): 661–672.
71. Chang JH, Yang X-F, Zempel JM, Rothman SM. The unilateral cobalt wire model of neocortical epilepsy: A method of producing subacute focal seizures in rodents. *Epilepsy Res*. 2004;61(1-3): 153–160.
72. Pitkänen A, Buckmaster PS, Galanopoulou AS, Moshé SL. Models of seizures and epilepsy. Academic Press; 2017.
73. Parthasarathy HB, Graybiel AM. Cortically driven immediate-early gene expression reflects modular influence of sensorimotor cortex on identified striatal neurons in the squirrel monkey. *J Neurosci*. 1997;17(7):2477–2491.
74. Rossi LF, Wykes RC, Kullmann DM, Carandini M. Focal cortical seizures start as standing waves and propagate respecting homotopic connectivity. *Nat Commun*. 2017;8(1):217.
75. Tobin WF, Weston MC. Focusing on the big picture: Induced focal seizures propagate along synaptic pathways. *Epilepsy Curr*. 2018;18(1):47–48.
76. Gertler TS, Chan CS, Surmeier DJ. Dichotomous anatomical properties of adult striatal medium spiny neurons. *J Neurosci*. 2008;28(43):10814–10824.
77. Kreitzer AC, Malenka RC. Endocannabinoid-mediated rescue of striatal LTD and motor deficits in Parkinson's disease models. *Nature*. 2007;445(7128):643–647.
78. Blumenfeld H. The thalamus and seizures. *Arch Neurol*. 2002; 59(1):135–137.
79. Cain SM, Snutch TP. Voltage-gated calcium channels in epilepsy. In: Noebels JL, Avoli M, Rogawski MA, eds. *Jasper's basic mechanisms of the epilepsies*. 4th ed. National Center for Biotechnology Information; 2012;66-84.
80. Connors BW. Initiation of synchronized neuronal bursting in neocortex. *Nature*. 1984;310(5979):685–687.
81. Detre JA, Alsop DC, Aguirre GK, Sperling MR. Coupling of cortical and thalamic ictal activity in human partial epilepsy: Demonstration by functional magnetic resonance imaging. *Epilepsia*. 1996;37(7):657–661.
82. Englot DJ, Morgan VL, Chang C. Impaired vigilance networks in temporal lobe epilepsy: Mechanisms and clinical implications. *Epilepsia*. 2020;61(2):189–202.
83. Paz JT, Davidson TJ, Frechette ES, et al. Closed-loop optogenetic control of thalamus as a new tool to interrupt seizures after cortical injury. *Nat Neurosci*. 2013;16(1):64–70.
84. Redecker C, Bruehl C, Hagemann G, Binus O, Witte OW. Coupling of cortical and thalamic metabolism in experimentally induced visual and somatosensory focal epilepsy. *Epilepsy Res*. 1997;27(2):127–137.
85. Westbrook GL. Seizures and epilepsy. In: Kandel ER, Schwartz JH, Jessell TM, Siegelbaum SA, Hudspeth AJ, eds. *Principles of neural science*. New York: McGraw-Hill; 2013:1116–1139.
86. Harden C, Tomson T, Gloss D, et al. Practice guideline summary: Sudden unexpected death in epilepsy incidence rates and risk factors: Report of the guideline development, dissemination, and implementation subcommittee of the American Academy of Neurology and the American Epilepsy Society. *Neurology*. 2017;88(17):1674–1680.
87. Asadi-Pooya AA, Nikseresht A, Yaghoubi E, Nei M. Physical injuries in patients with epilepsy and their associated risk factors. *Seizure*. 2012;21(3):165–168.
88. Turski L, Meldrum BS, Cavalheiro EA, et al. Paradoxical anticonvulsant activity of the excitatory amino acid N-methyl-D-aspartate in the rat caudate-putamen. *Proc Natl Acad Sci U S A*. 1987; 84(6):1689–1693.
89. Chkhenkeli SA. The inhibitory influence of the nucleus caudatus electrostimulation on the human's amygdalar and hippocampal activity at temporal lobe epilepsy. *Bull Georgian Acad Sci. Stereotact Funct Neurosurg*. 1978;4:406–411.
90. Chkhenkeli SA, Chkhenkeli IS. Effects of therapeutic stimulation of nucleus caudatus on epileptic electrical activity of brain in patients with intractable epilepsy. *Stereotact Funct Neurosurg*. 1997;69(1-4):221–224.
91. Velíšková J, Claudio OI, Galanopoulou AS, et al. Developmental aspects of the basal ganglia and therapeutic perspectives. *Epileptic Disord*. 2002;4:S73-82.
92. Garant DS, Gale K. Lesions of substantia nigra protect against experimentally induced seizures. *Brain Res*. 1983;273(1):156–161.
93. Chabardès S, Kahane P, Minotti L, Koudsie A, Hirsch E, Benabid AL. Deep brain stimulation in epilepsy with particular reference to the subthalamic nucleus. *Epileptic Disord*. 2002;4:83–93.
94. Benabid AL, Minotti L, Koudsié A, et al. Antiepileptic effect of high-frequency stimulation of the subthalamic nucleus (corpus

luysi) in a case of medically intractable epilepsy caused by focal dysplasia: A 30-month follow-up: Technical case report. *Neurosurgery*. 2002;50:1385–1392.
95. Benazzouz A, Piallat B, Pollak P, Benabid AL. Responses of substantia nigra pars reticulata and globus pallidus complex to high frequency stimulation of the subthalamic nucleus in rats: Electrophysiological data. *Neurosci Lett*. 1995;189(2): 77–80.
96. Zangiabadi N, Ladino LD, Sina F, Orozco-Hernández JP, Carter A, Téllez-Zenteno JF. Deep brain stimulation and drug-resistant epilepsy: A review of the literature. *Front Neurol*. 2019;10: 601.